NTNU

Norwegian University of
Science and Technology

The Influence of Polarization on the Wetting of Anodes in the Hall-Héroult Process

Ingrid Andersen Eidsvaag

Nanotechnology
Submission date: June 2016
Supervisor: Espen Sandnes, IMTE
Co-supervisor: Henrik Åsheim, IMT

Norwegian University of Science and Technology
Department of Materials Science and Engineering

For my bunny

Acknowledgments

I would like to thank SINTEF Materials and Chemistry for allowing me to use their experimental set-up for this project. In particular I would like to thank research engineer Henrik Gudbrandsen for his help with the troubleshooting and modifications of the wetting apparatus necessary for completing this work.

I am most grateful for the time my supervisors, Henrik Åsheim and Espen Sandnes, have spent helping me with the project. Their useful comments and suggestions on both results and presentation have been invaluable to me.

I would also like to thank Norsk Hydro ASA for providing me with sample anode material to test industrial anodes.

Finally I would like to thank Aksel Alstad at the NTNU mechanical workshop for machining and assembling the vertical and horizontal anodes used in the project.

Abstract

Improvements in the Hall–Héroult process for aluminium electrolysis has lead to a reduction in energy consumption from 20-25 kWh/kg Al 70 years ago, down to around 13-14 kWh/kg Al on average today. In order to further reduce energy consumption, it is important to look into bubble formation on the anode surface, and the shielding effect caused by this. The shielding of surface by the bubbles is amongst others related to how well the cryolite wets the anode surface.

In addition to reducing energy consumption, it is also necessary to look into reduction of emissions of greenhouse gases from the electrolysis process. One of the most important type of greenhouse gases produced in aluminium electrolysis is the perfluorocarbons. Perfluorocarbons are produced during anode effect, which may occur if the alumina concentration in the melt becomes too low. Though the exact mechanism causing anode effects is not known, it appears related to the ability of the electrolyte to wet the anode.

In this project, a lab scale electrolysis cell with a weight sensor on the anode was used to investigate trends in wettability during and after polarization both at normal operating voltages and at anode effect inducing ones. The electrolyte consisted of a cryolite melt with a cryolite ratio of 2.3 and 1 wt% Al_2O_3. Various anode designs and carbon in the form of graphite, glassy carbon and industrial pitch and coke were used.

It was found that both bubble coverage and average size of detaching bubbles decreased with increasing current density on the anode. This is believed to be mostly due to increased stirring of the melt caused by the extra bubbles formed. However, it is also possible that parts of the reduction came from improved wettability.

In addition, it was found that the wettability of anodes improved during polarization for normal operating voltages. A sizable fraction of the improvement in wettability occurred in the first few seconds of polarization, but it still took several minutes of polarization to obtain the best wettability. For voltages inducing anode effect, the wettability dropped quickly and a stable poor wettability is obtained already after a few seconds. This change preceded any changes in surface roughness of the anode, suggesting that it was caused by creation of CF-bonds on the surface. Testing with graphite, glassy carbon and industrial coke mixture revealed much the same trends in wetting behavior, however glassy carbon was much more resistant to anode effects and regained good wettability more quickly when polarized at normal operating voltages.

Contents

Introduction

Aluminium is one of the most abundant elements in the earth's crust, but due to its high chemical reactivity it is not found as an element in nature. Before the 19th century it was also difficult to synthesize large amounts of the metal [1], making it rare. The modern process for production of metallic aluminium is called the Hall-Héroult process [2]. It was patented by both Paul L. T. Héroult and Charles M. Hall independently in 1886. The process involves dissolving aluminium oxide (alumina) in another aluminium-salt with a lower melting point, and electrolyzing it to produce metallic aluminium. Development of this process, in combination with the Bayer process for production of alumina, lowered the cost enough to enable mass production of the metal.

The process behind aluminium electrolysis is still essentially the same as when it was developed, but the understanding and operation of the electrolysis cell has been greatly improved. This has resulted in a reduction in energy consumption in the electrolysis process from 20-25 kWh/kg Al 70 years ago, down to around 13-14 kWh/kg Al on average today [3], with some modern smelters consuming even less energy.

In order to further decrease energy consumption, it is important to look into bubble formation on the anode surface. The CO_2 produced will shield part of the anode surface, causing an increase in cell voltage. The coverage of bubbles on the surface will depend on how well the anode is wetted by the melt [4], and understanding wettability could thus be important to reduce energy consumption even further.

During recent years, more focus has also come to the effects on climate from industrial emissions of greenhouse gases. For aluminium electrolysis, the three main greenhouse gases emitted are [5]:

- CO_2 - typically around 80-90 % of emissions during normal operations
- CO - 10-20 % during normal operations, more during anode effects
- CF_4 - 10-15 % during anode effect

Of these three, CF_4 is the most potent, with a global warming potential of 6500 that of CO_2 and a life time in the atmosphere of several thousand years [6].

Although much research has gone into switching to inert anodes [7], aluminum electrolysis with carbon anodes is the only process used industrially today, and hence it is difficult to

reduce emissions of CO_2 substantially. On the other hand, formation of CF_4 and other perfluorocarbons (PFC) is a mostly unwanted side reaction of the cell, which, in addition to causing direct emissions, also disrupts the stability of the electrolysis cell.

It was previously believed that PFC could only be formed during a process called anode effect, where the cell voltage rapidly increases to high values. Recent studies do however show that PFC may also be generated in cells showing a normal cell voltage [8]. In both cases, PFC-formation is linked to low alumina concentration at the anodes.

Although the exact mechanism behind anode effect and PFC-formation is still unknown, it is clear that it is related to the wettability of the anode surface by the electrolyte. During anode effect, the wettability is lowered and a gas film is believed to cover the anode surface. Studies also suggest that the anode surface is permanently changed from anode effects, and that this change in surface might trigger new anode effects to happen more easily [9].

Varying current density through the anode has been shown to affect the wettability, though the results found from different experimental set-ups often vary [1]. In this study, a laboratory scale electrolysis cell with weight measurements of the anode is employed, to investigate how polarization affects the wettability of electrolyte-anode-systems for melts with low alumina content and various types of anodes. The experiment has been performed both at high voltages inducing anode effect and at normal operating voltages.

The work in this thesis builds on a specialization project of the same name, written in the fall of 2015 [10]. The specialization project gave information about changes in wettability after polarization, and after long anode effects, but did not give any information about the wetting and bubble behavior during polarization. These subjects will be treated more thoroughly in this thesis. The aim of this work is to gain fundamental knowledge on the wettability of the anode surface during electrolysis.

Theory

2.1 Wettability and wetting measurements

2.1.1 Interfacial tension and contact angles

Interfacial tension (γ) represents the energy required to expand an interface between two phases. It is defined as the derivative of the free energy with respect to the surface area (Equation 2.1).

$$\gamma = (\frac{\partial G}{\partial A})_{n,P,T} \tag{2.1}$$

In order to minimize the interfacial tension, liquids will minimize the surface area in contact with other phases. The interfacial tension depends on the chemical nature of the phases. The more chemically similar the phases are, the less energy is required to form an interface between them. Adding surface active ions can greatly change the interfacial tension between a liquid phase and another phase.

The contact angle is the angle observed on the contact point between a liquid, a solid surface and the surrounding gas. It is by convention measured into the liquid. This angle gives information about the wettability of the system. If the wetting angle is low, the liquid wets the surface well, and will spread out on it. If the angle is larger, the liquid does not wet the surface well, and will group together to form droplets. The contact angle under ideal and stable conditions is specific for the system, and is quantized by Equation 2.2, Young's equation [11].

$$\gamma_{sv} = \gamma_{sl} + \gamma_{lv} \cos\theta \tag{2.2}$$

In this equation, the γs represents the interfacial tensions between two different phases – s represents solid, v represents vapor and l represents liquid. θ is the measured contact angle. Hence, a large contact angle implies that the interfacial tension between solid and liquid is large compared to the interfacial tension between solid and vapor. This relation is sketched in Figure 2.1.

It should however be noted that the equilibrium angle referred to in this equation is rarely obtained, as very long time is required for equilibrium to be obtained.

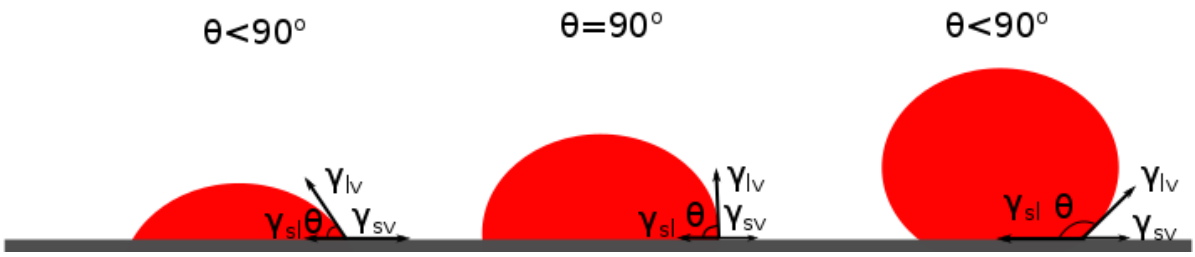

Figure 2.1: Wetting angles and surface tensions according to Young's equation.

In addition, as the surface is rarely completely smooth, a phenomena called static hysteresis is observed. In this case, one usually obtains a range of contact angles ranging between a minimum contact angle (referred to as the receding contact angle) and a maximum contact angle (referred to as the advancing contact angle). To understand the concept of advancing and receding contact angles one can imagine a droplet lying on a solid surface, its contact angle equal to the equilibrium one. If some more liquid is introduced slowly into the droplet it will grow, but the contact points with the surface will at first not change. Hence, the contact angle can increase until the advancing contact angle is obtained. Similarly one can remove liquid from the droplet without changing the contact point, until the receding contact angle is obtained. This effect can be rather large. Even for pure water on a smooth, homogeneous glass surface, the difference between the advancing and receding contact angle can be as much as 50-60^o [12].

The usual explanation for the observed hysteresis is that it stems from surface heterogeneity. This heterogeneity may be either chemical, physical or both. Hence, due to surface differences, the equilibrium angle may vary between points, and a range of macroscopic wetting angles may be observed. How surface roughness may affect the observed wetting angle is shown in Figure 2.2.

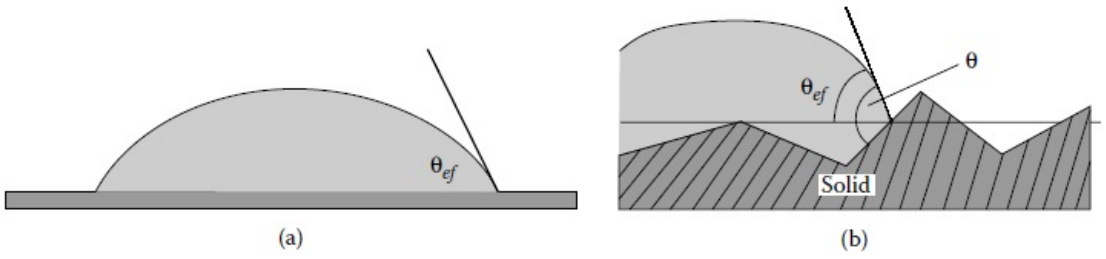

Figure 2.2: Observed (θ_{ef}) and actual (θ) surface angle for a (a) smooth and (b) rough surface. From [12].

When the contact angle is not the equilibrium value, the droplet may shift over the

surface, to attain the equilibrium value. When the angle is between the advancing and receding one, this motion will likely be very slow, possibly undetectable on a macroscale over the time span of the experiment. Larger deviations from the equilibrium value would give a more macroscopic movement, and hence a faster and more observable change in angle towards the equilibrium [12].

2.1.2 Immersion-emersion-method

The immersion-emersion-method is a method for measuring the contact angle between a liquid and solid. The solid is suspended from a load cell, measuring its weight. It is then lowered down into the liquid while position relative to surface and weight is recorded. The recorded weight now changes due to two forces – buoyancy (due to displacement of the liquid) and wetting. The total change in force observed is:

$$F = \gamma_{lv} p \cos\theta - V \Delta\rho g \tag{2.3}$$

where the first term comes from weight changes due to wetting and the second stems from buoyancy. In this equation γ_{lv} is the surface tension of the cryolite melt towards the gas, p is the perimeter of the solid being dipped into the liquid, θ is the angle between the liquid and the solid (Figure 2.3), V is the volume of displaced liquid, $\Delta\rho$ is the difference in density between the liquid and the gas, and g is the gravitational constant [11].

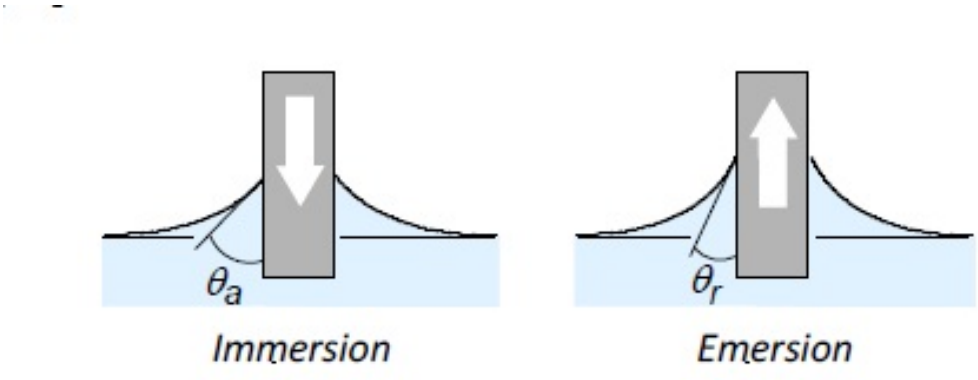

Figure 2.3: Principle sketch of wetting angle of less than 90^o during immersion and emersion. From [13].

Due to hysteresis, one expects to observe different contact angles going into and out of the melt. During immersion, the anode is pushed into the melt, and the movement of the meniscus along the surface may lag. Hence, a larger (advancing) wetting angle will be observed. During emersion, this works in the opposite direction, and a smaller, retracting angle is observed.

2.2 Aluminium electrolysis

Aluminium is produced industrially through the Hall-Héroult process. Alumina (Al_2O_3) is dissolved in an electrolyte comprised mostly of molten cryolite (Na_3AlF_6) at temperatures somewhat below 1000 °C. A cross-sectional scheme of a modern electrolysis cell can be seen in Figure 2.4. The sides of the cell have a ledge of frozen cryolite on them, to prevent molten cryolite from coming into contact with the internal lining of the cell and dissolving them. The shape and dimension of this ledge is highly dynamic and varies with the composition and temperature of the liquid phases. If the temperature is lowered too much, the ledge may extend far into the cell, thus blocking the current path, while too high of a temperature may cause the ledge to reduce thickness and in extreme cases disappear, causing wear of the side walls.

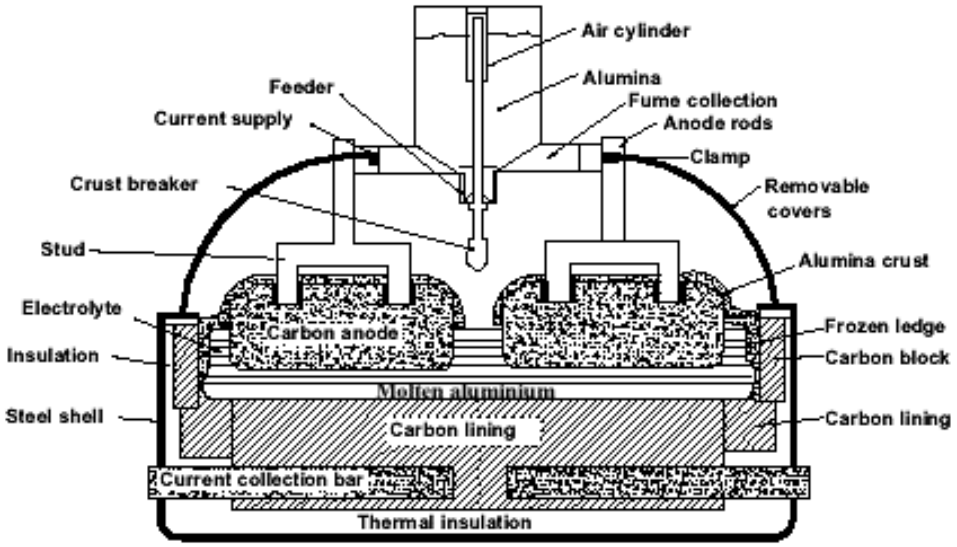

Figure 2.4: Cross-sectional scheme of an industrial Hall-Héroult cell. From [7].

During electrolysis, aluminium is produced at the cathode, while CO_2 and CO are produced at the anodes. Though the exact reaction steps are not fully known, the cathode reaction is believed to be reduction of AlF_4^- from the bath to Al and fluoride ions, while the anode reaction involves oxidation of complexes of aluminium, oxygen and fluoride. The sodium ions in the bath function as current carriers between the electrodes [14].

The two reactions for the cell are:

$$\frac{1}{2}Al_2O_3 + \frac{3}{4}C \rightleftharpoons Al + \frac{3}{4}CO_2, \qquad E_0 = -1.18 \text{ V} \tag{2.4}$$

$$\frac{1}{2}Al_2O_3 + \frac{3}{2}C \rightleftharpoons Al + \frac{3}{2}CO, \qquad E_0 = -1.07 \text{ V} \tag{2.5}$$

Though Reaction 2.5 is preferred thermodynamically, Reaction 2.4 occurs faster, and is the primary reaction except at very low current densities [15]. A modern electrolysis cell is operated with line currents of 300-500 kA, and a current density approaching 1 A/cm^2.

The current efficiency of aluminum production varies strongly between different smelter technologies, but the value is usually somewhere between 90 and 95 %. The loss in current efficiency during normal operations is mostly caused by the aluminum back reaction [16]:

$$\mathrm{Al} + \frac{3}{2}\mathrm{CO_2} \rightleftharpoons \frac{1}{2}\mathrm{Al_2O_3} + \frac{3}{2}\mathrm{CO} \tag{2.6}$$

Alumina is fed into the cell in small doses on regular time intervals. The goal of this is to keep the alumina content stable at around 2-3 wt%. Feeding too much alumina into the system leads to undissolved alumina lying on the cathode, disrupting the current flow. On the other hand, having too little alumina in the cell may cause an anode effect, in which the electrolyte is being electrolyzed and perfluorocarbons are formed.

2.2.1 Electrolyte composition

Cryolite (Na_3AlF_6) is the main component of the electrolyte (melt) in aluminium electrolysis. It is used due to its ability to dissolve large amounts of alumina and its relatively low melting point. The cryolite is not consumed during electrolysis, but small amounts may still disappear, for instance due to evaporation.

Several additives are usually also present in the electrolyte. The purpose of such additives is to improve the electrochemical properties of the electrolyte. The additives will reduce the melting point of the electrolyte, and hence also the required operating temperature of the cell, but they may also be there to reduce the energy consumption by reducing the electrical resistance of the electrolyte, reduce the solubility of metals or to reduce the vapor pressure, and hence increase the stability of the electrolyte [15].

The additives that are present in the highest concentration in the melt, in addition to alumina, are AlF_3 and CaF_2. In a normal electrolysis cell there will be around 10 wt% excess of AlF_3, 2-4 wt% of Al_2O_3 and 3-5 wt% of CaF_2 [17].

2.2.2 Anode material

From Equation 2.4, it is clear that the anode must be carbon based and consumable. The most basic components of the anode are petroleum coke aggregate and coal tar pitch used as a binder. These anodes are molded into rectangular shape, and then prebaked at high temperatures, before being put into the cell [15].

The anode voltage drop during normal operation is around 1.5-1.8 V, and of this, around 0.3-0.6 V is the anodic overpotential. Intentionally introducing dopants into the anode

will in some cases reduce the overpotential [18], however simply varying the type of coke used may also change the observed overpotential [19].

2.2.3 Bubble overpotential

The anodic overpotential consists of three different contributors – the reaction overpotential, the concentration overpotential and the bubble overpotential. The reaction overpotential is considered small at normal current densities [15], and the concentration overpotential is also assumed small due to stirring of the electrolyte caused by bubble formation. Hence, bubble formation is assumed to be the largest contributor to the overpotential.

The bubble overpotential can be understood as a reduction in effective surface area. During electrolysis, a large proportion of the anode surface is covered by the gaseous reaction products. As some of the surface is blocked by gas, the active surface area for electrochemical reaction is smaller than the geometric surface area. This will give an increase in current density for the active surface, which will cause a higher reaction overpotential [20]. How much of the surface is covered by bubbles depends on the process conditions, but several studies suggest that the bubble coverage may be as high as 20-50 % even during normal operation. Decreasing alumina content is found to increase the coverage of bubbles [15].

The presence of bubbles on the surface gives a higher resistance, which leads to an extra voltage drop of around 0.15-0.35 V [21]. This causes an unwanted increase in energy consumption. However, the motion caused by the bubbles detaching and rising to the surface is important in order to stir the electrolyte, and hence to ensure that alumina is being dissolved and supplied to the anode. Although Lorentz forces also induce some stirring in industrial cells, this effect is an order of magnitude less than the effect of bubble formation, and hence insufficient to mix the melt [22].

The bubbles nucleate at specific sites on the anode, and grow there until the drag force stemming from the movement of the surrounding melt is sufficient to overcome the interfacial force holding it in place [23]. They might then coalesce with other bubbles. The gas layer may subsequently grow, before rolling off the side of the anode. This process was documented by Zhao [21] on an anode with insulated side walls. The bubble development with a current density of 0.7 A/cm^2 is shown in Figure 2.5.

On industrial anodes this process happens several places at once, while at smaller experimental anodes the effect is more sequential, and a certain periodicity can be observed [20].

The growth of bubbles is influenced by the ability of the electrolyte to wet the anode. If the wetting is good, less of the surface will be covered by gas bubbles, and bubbles will detach quickly, without requiring further growth [24].

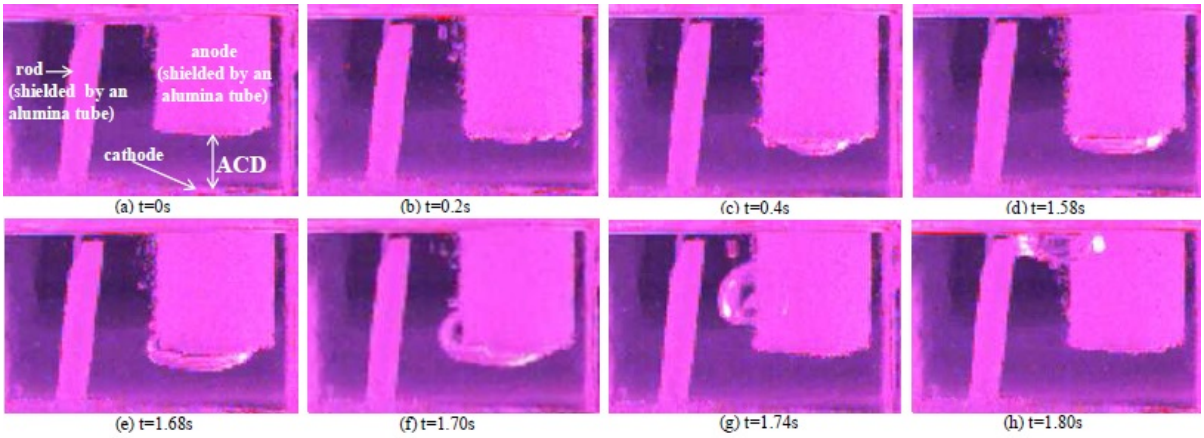

Figure 2.5: Bubble morphology in a life cycle. From [21].

Cassayre [25] observed that the diameter of gas bubbles detaching from a graphite anode were usually around 2-3 mm in diameter. With increasing current density it was observed that the bubbles were smaller, but were created at a higher frequency. This was attributed to the increased stirring effect caused by the extra gas production. Lower alumina concentration in the melt appeared to favor larger bubbles. Zhao [21] observed a decrease in total bubble coverage with higher current density. Also this was believed to be due to improved stirring.

2.2.4 Wettability of cryolite and carbon

The wetting of the anode by cryolite depends on the interfacial tension between the three phases gas, cryolite and anode carbon, through Young's relation shown in Equation 2.2. The contact angle for cryolite-carbon-systems at 1011 °C has been found to be between 121° and 144° for graphite, and somewhat lower for amorphous carbon [1]. The angle decreases with increasing temperature. Addition of other components into the cryolite, may also affect the wetting angle. In general, the angle appears to not be strongly affected by addition of AlF_3 or CaF_2, while addition of Al_2O_3 decreases the contact angle [1, 26]. As the alumina content of the melt increases, the dominant Al-O-F-specie in the melt changes from $Al_2OF_8^{4-}/Al_2OF_6^{2-}$ to $Al_2O_2F_4^{2-}$. This could have an effect on the interfacial tension of the system, and hence on the wetting [27]. Doping of the anode itself has also been shown to affect the wettability, though it is unclear if this is due to changes in the carbon material, or due to the dopants being dissolved in the melt, affecting its surface properties [18].

Polarization of the anode also has a large effect on the wettability. Passing current through the anode appears to have a positive effect on the wettability for moderate current densities, while a current density high enough to induce anode effect diminishes the wettability. This behavior is strongly dependent on the alumina content in the melt

[1].

2.2.5 Anode effect

Anode effects occur under conditions where the alumina content of the electrolyte becomes too low and the electrolyte itself starts to undergo electrolysis. The cell voltage rises abruptly to higher values due to the fixed line currents used in industry and substantial amounts of CO, CF_4 and C_2F_6 are formed. During anode effect the electrolyte will be strongly dewetting with respect to the anode, and a continuous gas film will cover the anode surface. Industrially, an anode effect is usually defined as having a voltage of more than 8 V for a consecutive time of more than three seconds, though some smelters may define it differently [8]. The reactions for PFC-formation are shown below.

$$AlF_3 + \frac{3}{4}C \rightleftharpoons Al + \frac{3}{4}CF_4, \qquad E^o = -2.58 \text{ V} \tag{2.7}$$

$$AlF_3 + C \rightleftharpoons Al + \frac{1}{2}C_2F_6, \qquad E^o = -2.80 \text{ V} \tag{2.8}$$

It is also thermodynamically possible that the reaction on the anode surface is creation of COF_2 through Reaction 2.9, and that the product then decomposes to CF_4. This reaction path is somewhat disputed, as COF_2 is seldom detected in experimental set-ups [28].

$$\frac{1}{2}AlF_3 + \frac{1}{4}Al_2O_3 + \frac{3}{4}C \rightleftharpoons Al + \frac{3}{4}COF_2, \qquad E^o = -1.88 \text{ V} \tag{2.9}$$

As the voltage is much higher than under normal operating conditions, anode effects leads to excessive heating of the cell, which again leads to melting of the side walls, and thus to instability.

The mechanism behind anode effect is still not fully understood, and several different suggestions for mechanisms have been proposed. Two of the proposed mechanisms are (1) diminishing wettability due to decreasing alumina content and (2) formation of adsorbed surface compounds that may either insulate the surface or diminish its ability to be wetted by cryolite. The surface compounds could be chemisorbed fluorine or oxygen compounds or even adsorbed CF_4-gas [1]. Poorer wetting of the surface makes gas bubbles formed during electrolysis grow larger and stay longer on the surface, thus insulating a larger part of it. This will increase the current density in other parts of the anode, and hence the overvoltage [18].

In laboratory experiments, the current density appears to be an important factor for determining when an anode effect occurs. Depending on the melt and anode, it is usually

possible, even at low alumina concentrations, to pass some current through the system without triggering an anode effect. The lowest current density necessary for onset of anode effect is referred to as the critical current density (ccd). The critical current density for onset of anode effect is increasing with increasing alumina content, from around 0.1 A/cm^2 in pure cryolite to several A/cm^2 in saturated melts [15].

Changing the geometry and type of anode material affects the ccd strongly. Anodes with more vertical surface area exhibit a higher ccd. This is likely due to the gas being able to roll off the surface more easily, ensuring more active surface area at a given time. Changing the type of anode to one giving a more uniform current distribution could also increase the ccd. Some studies suggest that anode effects cause changes to the physical or chemical structure at the surface of the anode which enables new anode effects to occur at a lower current density than before [1, 9].

In industrial cells, one anode going into anode effect will cause increased current load on the remaining anodes in the cell. This may cause a domino effect, in which the anode effect within seconds propagates to the other anodes of the cell, causing a full scale anode effect [29]. When an anode effect occurs industrially, it is attempted suppressed by feeding large amounts of alumina into the cell at once, and by moving the anodes down and up again (so called anode effect quenching). Movement will expose fresh surface to the melt and temporarily short circuit the cell, if the anodes come into contact with the metal. The movement also induces stirring in the cell. Stirring can also be achieved manually, by adding wooden poles into the cell.

Though it was previously believed that PFC-formation only occurred during full scale anode effects, newer research has shown that PFC-formation in industrial cells may also occur during what appears to be normal operating conditions. This phenomena has by some been termed non-anode-effect (NAE) PFC-emissions. For Chinese smelters investigated, NAE PFC-emissions was found to cause 70 % of the total PFC-emissions [30]. The NAE emissions are put into two categories – low voltage propagating anode effects and nonpropagating anode effects. For the low voltage propagating anode effects, the anode effect occurs at one anode and then spreads to surrounding anodes due to increased current load on these, just like with a normal anode effect. The difference between these anode effects and full scale ones is that the effect only occurs in parts of the cell, with other parts operating normally. The nonpropagating anode effects do not spread to other anodes [29].

Though this PFC-generation happens at lower voltages than what is considered an anode effect by the industrial definition, the fundamental mechanism behind is believed to be the same. These effects are also thought to be linked to low concentrations of alumina, but now only in a localized part of the cell. NAE emissions are believed to contribute to a larger fraction of total emissions in modern high amperage cells. These are often larger, with a smaller interpolar distance, which again enables large concentration differences across the cell [8].

2.2.6 Surface changes of anode due to anode effect

Anode effects may also have more permanent effects on the surface of the anode, by changing the structure, so that the wetting is still diminished, even after the anode effect is over. This is believed to be due to formation of a fluorocarbon film with low surface energy on the surface of the anode [31].

Figure 2.6 shows SEM-imaging of two anodes that have undergone normal electrolysis (left) and extended anode effect (right). According to these findings, the bottom and edge parts of the anode surface is smoother after the prolonged anode effect. This is attributed to an electropolishing effect due to high current densities in these areas. XPS-analysis of the same region revealed the presence of bonds between carbon and fluorine on the anode surface, which could diminish the wetting ability of the anode. These bonds were still present after the anode effect had been suppressed and the anode was removed from the cell [32].

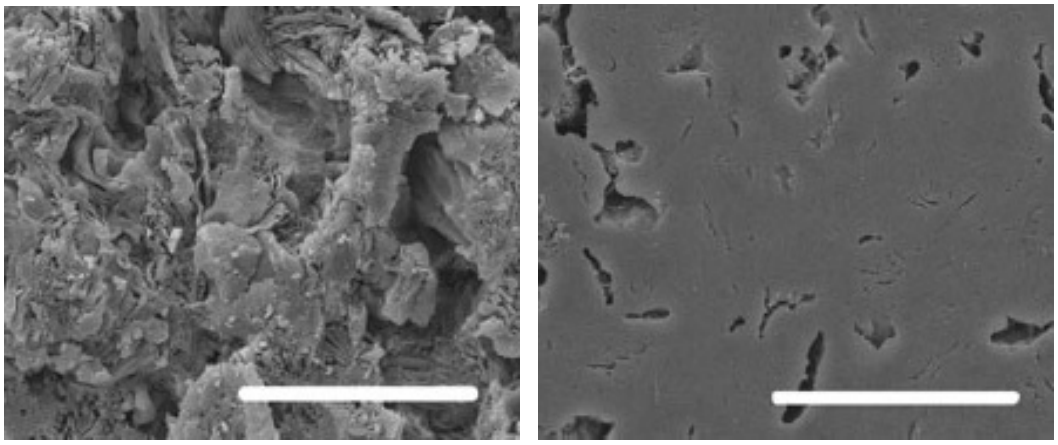

(a) After normal electrolysis (b) After extended anode effect

Figure 2.6: SEM images of surface of anode after normal electrolysis and AE. Scale bar is 50 μm. Adapted from [31].

2.3 Previous results with the wetting apparatus

Work was conducted on wettability of graphite anodes during polarization in the fall of 2015. This was done in a specialization project on the same topic as this thesis [10]. All experiments were conducted using a melt with a cryolite ratio of 2.3, an alumina content of 1 wt%, and a temperature of 1000 °C. This study revealed the following trends:

- Polarization at voltages low enough for normal electrolysis to take place improves the wettability of the carbon surface. After several polarizations, the wettability appears to stabilize at a maximum value.

- When an anode effect occurs, the wettability of the anode surface is reduced quickly.
- Both for normal electrolysis and anode effects, the obtained changes in wettability appears to be constant. In these experiments, the wetting weights remained constant for more than an hour after polarization or until another polarization was applied.
- The voltage required for inducing an anode effect varies. If the last polarization on the anode induced an anode effect, the voltage required to induce another one is reduced.

Methods

3.1 Description of wetting apparatus

The wetting apparatus used in this experiment is a slightly modified version of an apparatus built and tested by SINTEF during 2012-2013. This apparatus is described in detail in [13]. Most of the setup is still the same, but the load cell has been moved outside, to the top lid of the cell. The rod which the anode hangs from is suspended from a metal string that passes through a hole in the top of the apparatus up to the load cell. The hole is covered in vacuum grease, to reduce air flow into the apparatus. Additionally the thermocouple inside the cell has been removed, to reduce noise on the weight sensor. A sketch of the upper parts of the apparatus in its current state can be seen in Figure 3.1.

The apparatus consists of a water cooled cylindrical furnace equipped with a step motor (ROBO Cylinder RCP2W-RA4C-I-42-P-5-150-P1-M-B) in the bottom to allow the crucible containing the melt to be raised and lowered while its position is logged. This allows the anode to be immersed into the melt in a controlled fashion during experiments. The furnace is heated by a power supply, allowing it to reach the operating temperature of 1000 °C. The apparatus is mounted on a freestanding aluminium frame, to reduce vibrational noise from other machinery present. All wires going into and out of the furnace are attached to the frame, to keep them stable. A gas stream of argon is fed through the cell from the top, and flows through it, to ensure that the furnace is kept under an inert atmosphere. The temperature in the furnace is measured at the level of the cathode crucible, by a thermoelement. It is also possible to have a second thermocouple suspended from the top of the cell when extra measurements are needed. The anode is suspended from the top by a steel rod hanging from a load cell (FUTEK LSB210). The signal of this load cell is logged by a microcontroller (FUTEK IMP650). Extra weights can be added on top of the anode, to improve stability and ensure that it stays leveled. To do polarization, the anode and cathode are connected to a HP 6032A power supply. The power supply can be operated to either give a constant current or a constant voltage. When running constant current, the maximum voltage is set to 20 V. During the constant voltage mode the maximum current output is set to 50 A. After going through the cell, the current passes through a shunt resistor with a resistance of 0.01 Ω to log the current. Both current and cell voltage are logged by a NI cDAQ 9174

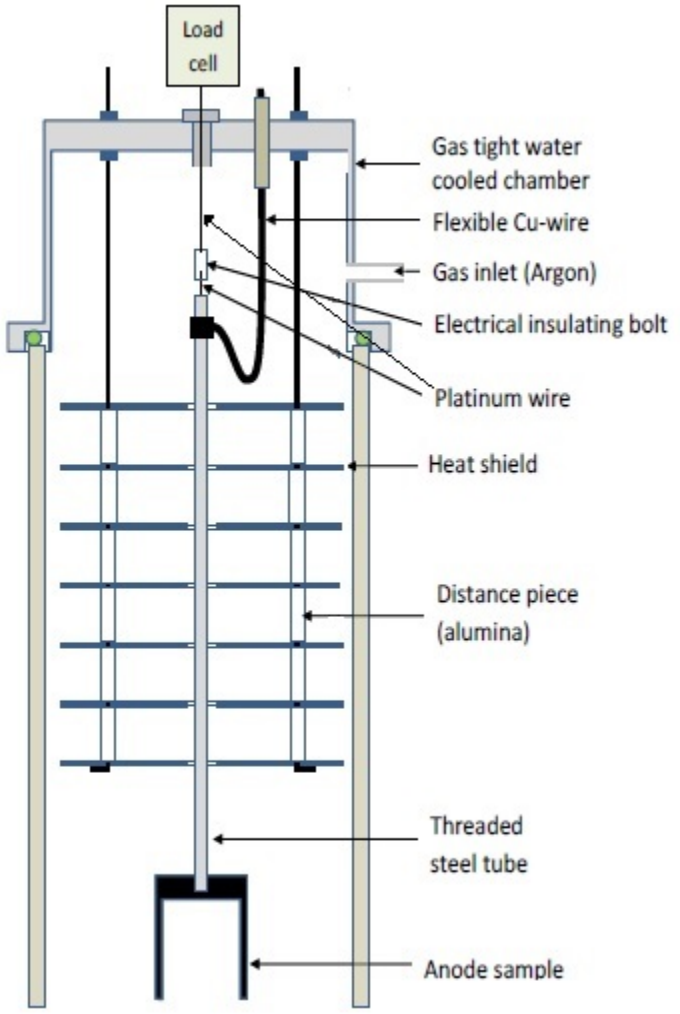

Figure 3.1: Sketch of the upper part of the wetting apparatus. Adapted from [13].

with a NI9205 module. Before the logger, the voltage is reduced using a voltage divider. With this setup, the logger can read voltages up to around 30 V.

3.2 Anode materials

Three types of anode material was used in this project, graphite, glassy carbon and an industrial coke/pitch mixture supplied by Norsk Hydro ASA.

Three general shapes of anodes were used. The three forms were cup anodes, horizontal anodes and vertical anodes. The cup anodes were used when a large perimeter was needed, the horizontal ones were used for observing bubble development on the anode surface and the vertical ones were used when it was necessary to reduce the noise from

bubbles resting on the surface.

3.2.1 Cup graphite anode

The anode is a hollow cylinder with 30 mm outer diameter, and wall thickness of 2 mm. The height of the anode is 5.5 cm. It is made of graphite with a density of 1.771 g/cm^3. The top of the anode has two holes in it, to allow gas to escape from the inside, and a tapered hole in the middle, to attach it to the steel rod hanging from the load cell. Pictures of the anode can be seen in Figure 3.2. It is manufactured by Schunk Tokai Scandinavia AB.

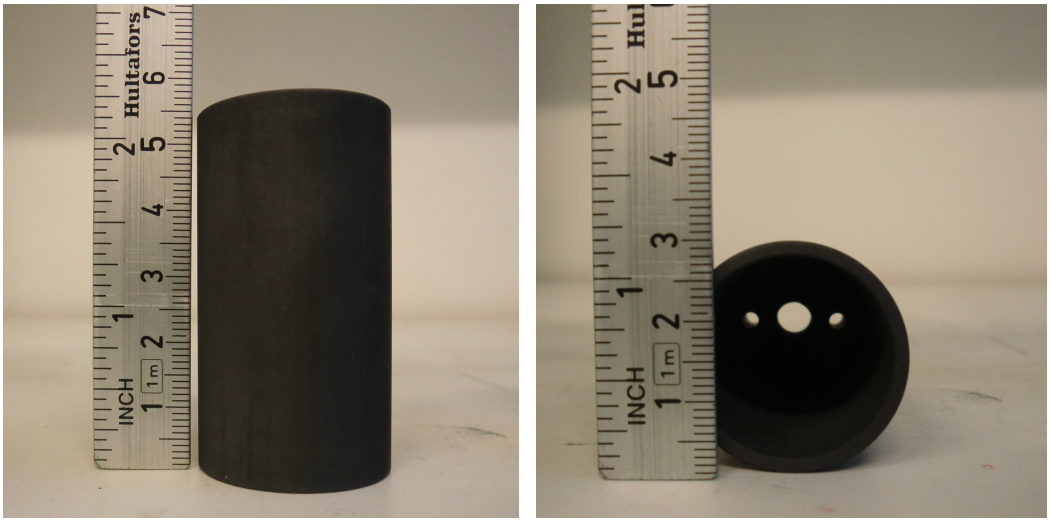

(a) Seen from the side (b) Seen from the bottom

Figure 3.2: Images of the cup graphite anode.

3.2.2 Vertical graphite anode

The vertical anode consists of several cylinders with the same diameter fastened together on a threaded graphite rod. The lower cylinder is made of boron nitride, which is nonconductive, and hence does not take part in the electrolysis process. This cylinder is 11 mm high. On top of this, there is another cylinder of graphite. The height of this section can be either 7 mm, 10 mm or 30 mm. On top of the carbon layer is another 15 mm cylinder of boron nitride, followed by a final layer of carbon, 15 mm high. The diameter of the cylinders were either 16 mm or 22 mm. The cylinders with 16 mm diameter had a carbon layer height of either 7 mm or 10 mm, the larger ones had either 10 mm or 30 mm tall carbon surface. A picture of one of the anodes can be seen below in Figure 3.3. The graphite parts have the same density as the cup, 1.771 g/cm^3, and are also manufactured by Schunk Tokai Scandinavia AB.

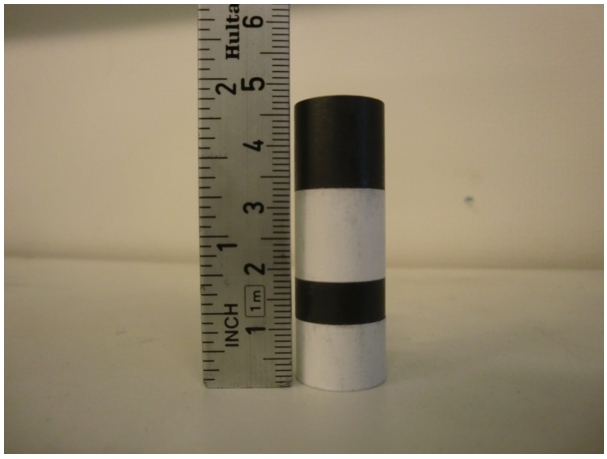

Figure 3.3: Side view of vertical anode with a 7 mm carbon section.

3.2.3 Horizontal graphite anode

The horizontal anodes were made of a hollow cylindrical shell of boron nitride, with a core of carbon on the inside. This ensures that only horizontal surface is available for reactions. The boron nitride layer has an outer diameter of 22 mm, and the carbon core has an outer diameter of 16 mm. The entire structure has a height of 30 mm. A picture of the anode can be seen below in Figure 3.4. The graphite part is the same as was used for the vertical anodes.

To improve bubble release from the surface, the BN layer on the side was cut down to an angle of approximately 45^o. This is not shown in the picture.

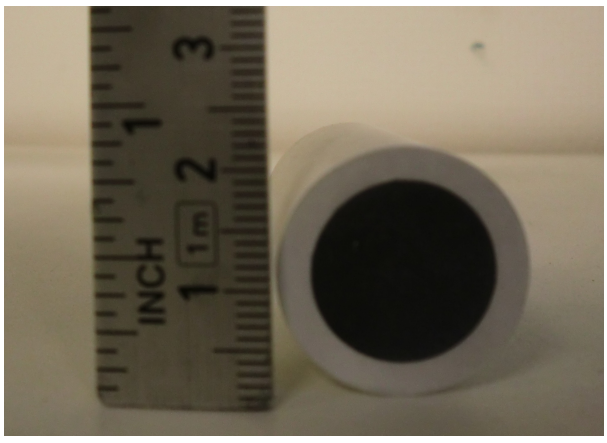

Figure 3.4: Bottom view of horizontal anode.

3.2.4 Glassy carbon

One anode of glassy/vitreous carbon [33] was used. The anode was shaped as a cup similar to the anodes described in Section 3.2.1. The outer wall diameter of 3.9 cm and a wall thickness of 2.25 mm. The density of the carbon material was 1.5 g/cm^3.

3.2.5 Industrial anodes

The carbon material from the industrial anodes was supplied by Norsk Hydro ASA. The anode material consists of 15 % pitch and 85 % coke. The diameter of the coke particles ranged between 0 and 6 mm, with 53 % of the particles being smaller than 1 mm. This anode was specially made for lab purposes, and does not have the same coke aggregate composition and pitch content as anodes used in the industrial electrolysis cells.

The carbon material was shaped into vertical anodes with 22 mm diameter. The active carbon part was 10 mm tall for some anodes and 30 for others. All other parts of the anodes were the same as for the thick vertical graphite anodes described in Section 3.2.2.

3.3 Preparation of cryolite melts

The cryolite melt is prepared by mixing cryolite (Sigma-Aldrich, purity > 97 %, alumina content = 1.04 wt%), γ-aluminium oxide (Merck) and aluminium fluoride (Alcoa, sublimed in-house). All the melts are prepared with a cryolite ratio (n_{NaF}/n_{AlF_3}) of 2.3 and a starting concentration of alumina of 1 wt%.

The salts are mixed and placed in a carbon crucible with inner diameter 7.5 cm. In some of the experiments, the crucible has a hollow cylinder of Si_3N_4 on the inside, to prevent current from the anode to go to the side walls of the crucible. The crucibles can be seen in Figure 3.5.

3.4 Processing of data

The wetting apparatus logs the total weight change during the experiments. However, the largest part of this weight change does not come from wetting, but rather from buoyancy, and other effects. Hence, in order to get information about the wettability, the other effects must be compensated for. How this is done is described below.

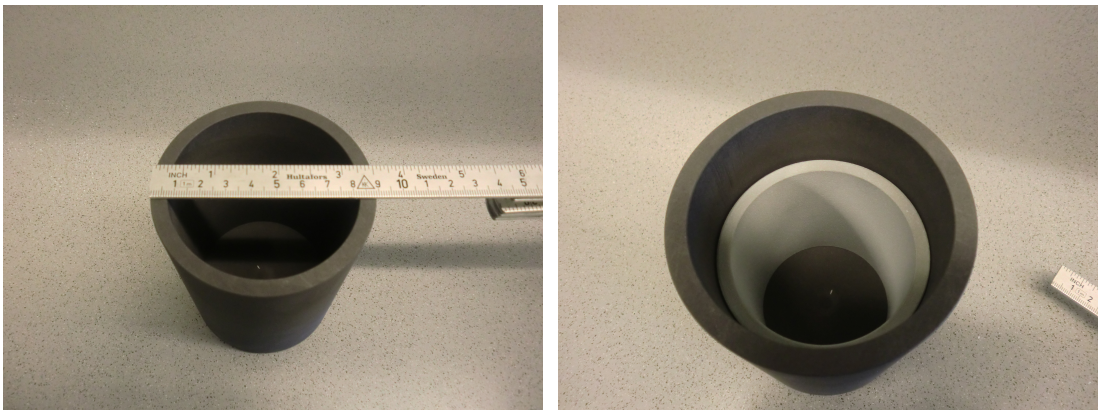

(a) Without shielding (b) With shielding

Figure 3.5: Images of the crucible without (a) and with (b) the shielding cylinder.

3.4.1 Determining contact point

As the melt is not visible during the experiment, the contact point between the liquid has to be determined using other methods. The two parameters that change notably at the contact point is the weight of the anode and, when the anode has previously been polarized, also the measured cell voltage. When both of these showed a clear jump at the contact point, an average between the two values was used, otherwise only the value from weight change was used. The difference between the calculated contact points from these two methods is usually less than 0.2 mm.

In the case where the weight increased initially, the contact point was set to be the point at maximum weight. For the case where the weight did not do a jump upwards, the contact point was set to be the last point where the weight of the anode was the same as in air.

Examples of where the contact point was determined to be in the two cases described above can be seen in Figure 3.6.

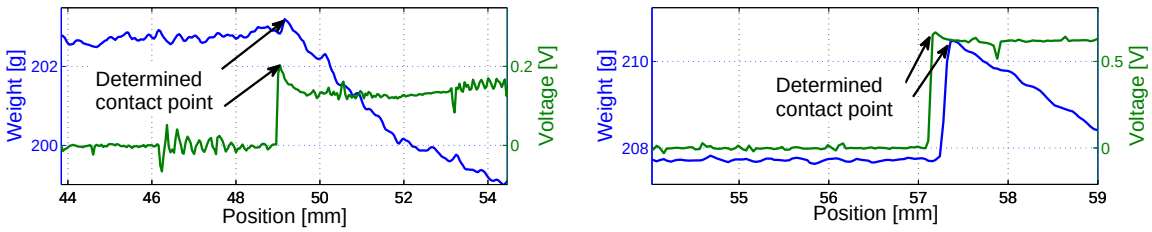

(a) Without weight jump (b) With weight jump

Figure 3.6: Examples of determined contact points based on the method mentioned in Section 3.4.1.

3.4.2 Calculating weight correction factor and removing buoyancy effects

The expected weight change due to buoyancy can be calculated from the second part of Equation 2.3.

$$F_{buoyancy} = -V\Delta\rho g \tag{3.1}$$

For a melt with 1 wt% of Al_2O_3 and a cryolite ratio of 2.3, the density is approximately 2.045 g/cm^3, and the density of air is assumed to be around 0.001 g/cm^3. Hence the apparent weight change due to buoyancy for the cup graphite anodes is:

$$\Delta m_{buoyancy} = -V\Delta\rho = -3.60 \text{ g/cm} \times h \tag{3.2}$$

where h is the immersion depth. As the liquid level increases as the anode is immersed, h is slightly larger than the distance the anode has traveled into the melt. Adjustments for other kinds of anodes are done by changing the immersed volume V accordingly. The melt density is adjusted according to a table when other alumina concentrations are being used.

After removing the effect of buoyancy, one is left with plots similar to the lower ones in Figures 3.7 and 3.8. In Figure 3.7 the buoyancy corrected weight is plotted vs. time, while it in Figure 3.8 is plotted vs. position. For a previously unpolarized graphite anode, one expects a fairly homogeneous surface, and hence a stable buoyancy corrected weight change during immersion, as is observed in the following images.

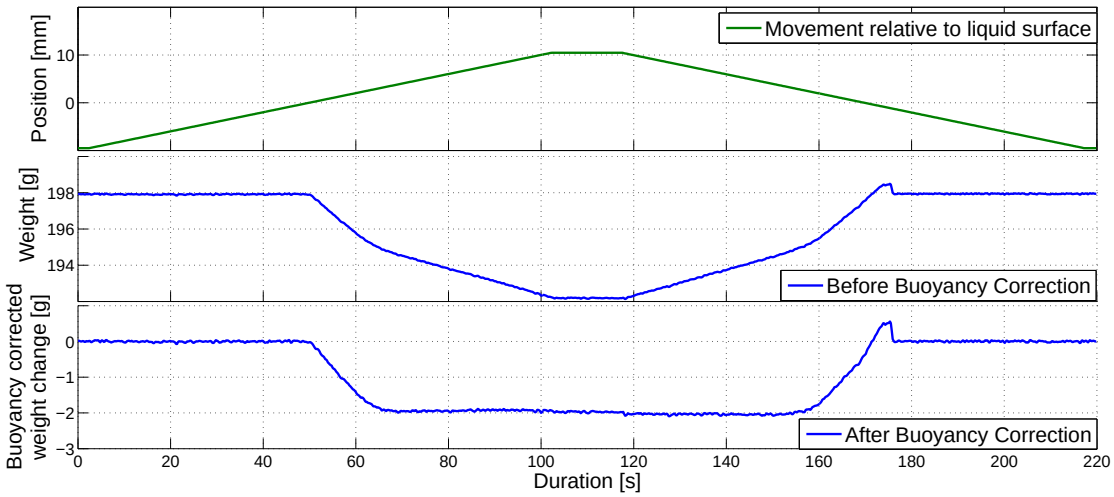

Figure 3.7: Plot of weight vs. time for an immersion to 10 mm at a speed of 0.2 mm/s before (mid) and after (lower) buoyancy correction has been applied. Upper plot shows position of anode relative to melt. Positive position means that the anode is immersed in the melt.

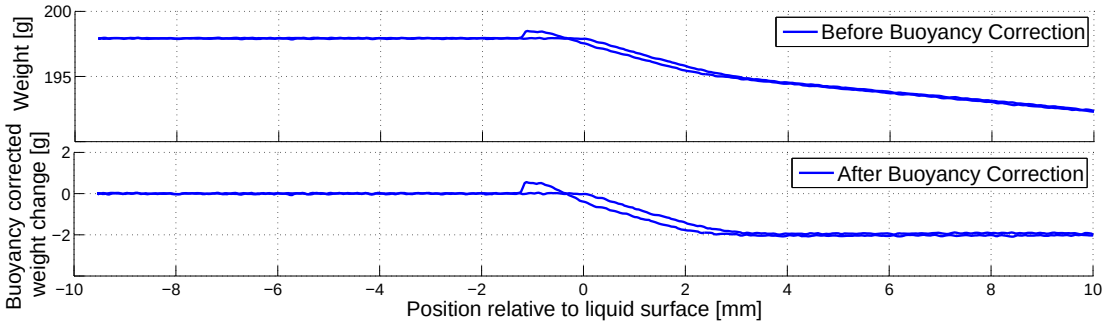

Figure 3.8: Plot of weight vs. position for an immersion to 10 mm at a speed of 0.2 mm/s before (upper) and after (lower) buoyancy correction has been applied. Positive position means that the anode is immersed in the melt.

3.4.3 Compensating for carbon consumption

When current passes through the anode, some carbon will be consumed. This means that the effect of buoyancy will be smaller with time, as less volume is immersed into the melt. To compensate for this, it is assumed that one mole of carbon is consumed for every four moles of electrons passing through the cell. This holds if only CO_2 is produced at the anode. With coproduction of CO, the consumption will be higher than what is assumed here.

The consumption of carbon is translated into a volume change of the active anode by assuming a density of graphite of 1.771 g/cm^3, and the buoyancy correction term is adjusted accordingly. This adjustment is done after each run.

3.4.4 Compensating for material deposition

During the course of a dip, some of the melt will evaporate. As the temperature higher up in the system is lower, the matter may solidify again and deposit on available surfaces. As some matter deposits on the rod holding the anode, the weight of the anode will increase slightly for each experiment. To compensate for this, the weight of the anode hanging above the melt before and after an immersion is compared. If the weight differs, this is compensated for by assuming that the weight increase occurs at a stable rate during one immersion and this increase is then subtracted from the measured weight.

3.4.5 Presenting weight change data

When the weight changes for several runs are presented, three different values are usually given – the buoyancy corrected weight during polarization, after polarization and after

retraction and reimmersion. The plot of Figure 3.9 exemplifies how these values are obtained. After correcting for buoyancy, one gets a plot looking similar to the one below. Here, the anode was immersed into the melt to a given point, held there for 120 s, polarized for 60 s and then held in position for 180 s more.

The data points which would give the values for "during polarization", "after polarization", and "after reimmersion" are shown below. In the case when a value is not stable during the entire period (the weight during polarization is for instance often observed to be slowly increasing), only the last few data points are used.

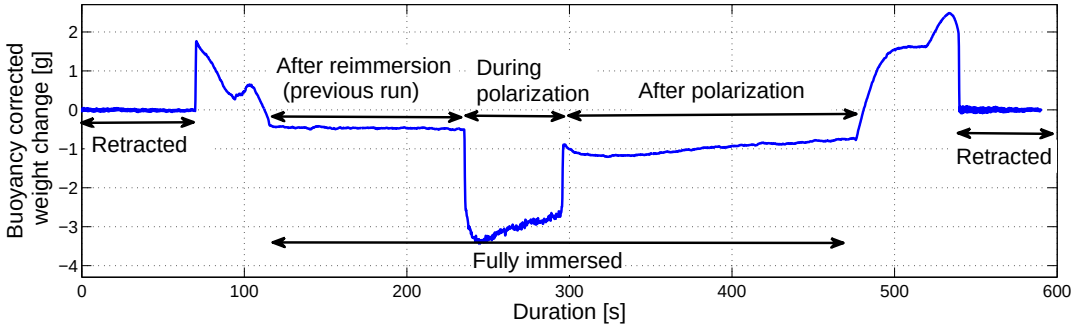

Figure 3.9: Plot of buoyancy corrected weight change vs. time. Polarization lasted for 60 s. The double arrows indicate where the values of buoyancy corrected weight during polarization, after polarization and after reimmersion are taken from.

The measured buoyancy corrected weight change found in these experiments will vary between the different types of anodes, as perimeter length of the different anodes vary. To enable comparison of data from different anode types, the buoyancy corrected weight change will be divided by the perimeter length of the anodes when it is presented. This will give the same value for different anodes, when the wetting is equal. This will be done for the plots in the Results Section. The perimeter length is found by assuming the surface to be completely smooth. Due to surface roughness, the actual perimeter is somewhat larger than this, however this should not affect the resulting wetting weight to a large extent.

The allowed range for equilibrium wetting weight for the system is approximately between -0.109 and 0.109 g/cm for a melt with a cryolite ratio of 2.3 and 1 wt% alumina at 1000 ^{o}C. The corresponding wetting angles for the range of allowed wetting weights is shown in Figure 3.10.

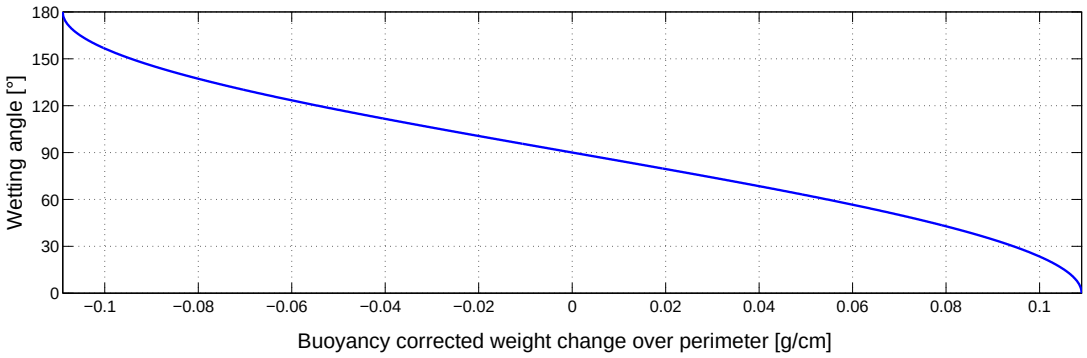

Figure 3.10: Corresponding wetting angles for the allowed wetting weights.

Measurement sequences

All the melts used initially had a cryolite ratio (n_{NaF}/n_{AlF_3}) of 2.3 and a starting concentration of alumina of 1 wt%. The temperature during experiments has been kept steady at 1000 °C for the entire duration. All movements were done with a speed of 0.2 mm/s.

The following sections gives information about the sequences used in measurements. The exact sequences are included to make it possible to reproduce the experiments. This does however make the sections rather heavy to read. Readers who do not wish to reproduce some of the experiments are advised to not spend too much time on these sections, but rather to come back to and read specific parts if something is unclear in the results.

4.1 Investigating reproducibility

4.1.1 Repeated procedure

To test reproducibility, the same experimental procedure was performed on three different cup graphite anodes. The side walls of the crucible were shielded, to give an even current distribution between the inside and outside of the anode.

The procedure was as follows: The anode was held 10 mm above the melt for 30 s. It was then immersed 10 mm into the melt, held there for 120 s, polarized for 60 s and then held there for 180 s more before it was retracted at the same speed. The starting voltage was 1 V, and the voltage was increased in 1 V increments until 10 V. The entire procedure was repeated twice. The procedure is summarized in Table 4.1.

4.1.2 Reaching equilibrium wettability

A test was conducted to observe whether the equilibrium wettability can be observed during experiments. First, the anode was immersed 10 mm into the melt and held there for 600 s. This gave the advancing wettability. After this, the anode was immersed to 15 mm, and then retracted back to 10 mm and paused for 600 s. This gave the receding wettability.

Table 4.1: Sequence used for voltage ramping to test reproducibility

Step no.	Position relative to surface [mm]	Movement speed [mm/s]	Wait time [s]	Voltage [V]
1	-10	-	30	0
2	10	0.2	120	0
3	10	-	60	1/2/../10
4	10	-	180	0
5	-10	0.2	30	0

The measurement was repeated three times – first it was done on a previously unpolarized anode, then it was tested on an anode which had been polarized with 3 V for 300 s on 10 mm, and then it was repeated after the anode had been polarized at an anode effect inducing voltage of 25 V for 600 s.

4.2 Increasing alumina concentration

A test was conducted on a graphite cup anode to see how the wetting changed with alumina content at a surface which had undergone long anode effect and at a surface which had been polarized on normal operating voltages.

First, an area up to 20 mm was polarized with an anode effect inducing voltage of 20 V for 10 minutes, to ensure poor wetting there. After this, the area up to 10 mm was polarized at 3 V for five minutes, to improve wetting in this lower part.

The wetting was then measured by immersing the anode first to 5 mm, then holding it in position for 300 s, then immersing it to 15 mm into the melt and again holding it there for 300 s. After retracting the anode again, alumina was added to increase the total concentration to 2 wt%. The anode was held above the melt during alumina addition and for some minutes after, but was afterwards immersed again using the same sequence to measure the wetting again. After each measurement, more alumina was added, always increasing the total alumina content with one percent. This was repeated until the melt was fully saturated with alumina.

4.3 Bubble development on horizontal anodes

To test bubble development on horizontal surfaces, the horizontal anode described in Section 3.2.3 was used. The intent was to check how the bubble size changed with changing current density.

The setup was run with a constant current, and the voltage and weight response was recorded.

The anode was immersed 10 mm into the melt, held there for 60 s without current passing through, then polarized for 60 s and then held there for 60 s before taking it out again. This was repeated for several different average current densities, ranging from 0.25 A/cm^2 to 8 A/cm^2. This sequence is shown in Table 4.2.

Table 4.2: Sequence used for current controlled experiments on horizontal surfaces

Step no.	Position relative to surface [mm]	Movement speed [mm/s]	Wait time [s]	Current density [A/cm^2]
1	-10	-	30	0
2	10	0.2	60	0
3	10	-	60	0.25/0.50/../8.0
4	10	-	60	0
5	-10	0.2	30	0

Three different values are reported for the bubble development. First, the total amount of bubbles during the 60 s polarization is found, by counting the amount of weight jumps upwards during the polarization. Second, the average weight change when a bubble detaches is reported. Third, a sharp drop in weight is observed at the start of the polarization, correlating to the total volume of gas at the surface. This weight is also reported. These three values are shown as (1), (2) and (3) in Figure 4.1.

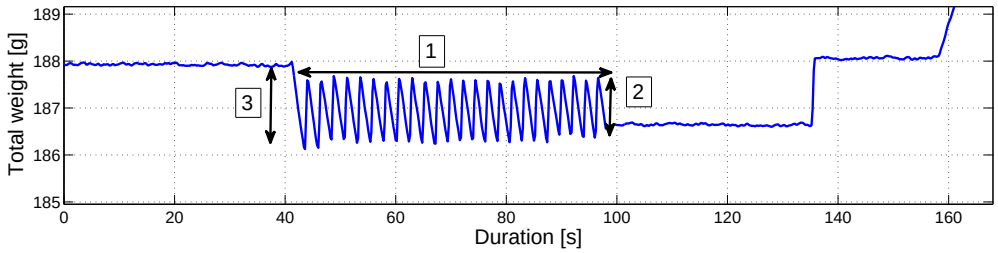

Figure 4.1: Reported values for the horizontal anode setup

4.4 Observing movement of the meniscus

The vertical anodes were introduced to attempt to observe how the meniscus moved during normal polarization. Due to extensive bubble development on the cup anodes, it is not possible to see if the meniscus moves upwards continuously during polarization, or if all improvement in wetting occur after the polarization has finished. Using anodes

with no horizontal carbon surface should reduce the bubble development sufficiently to observe changes also during polarization.

To observe movements of the meniscus during polarization, a vertical graphite anode with a 7 mm tall active carbon area was used. The change in meniscus was measured both on the carbon phase (immersed 15 mm) and on the second boron nitride phase (immersed 25 mm).

To measure changes in meniscus, the anode was immersed into the melt to the intended spot. It was then held there for 60 s to stabilize, before it was polarized for 300 s. After polarization it was held in place for 180 s before being retracted.

Between each of the measurements, the anode was immersed 25 mm into the melt so that the entire carbon phase was immersed, and was subjected to anode effect inducing voltages for more than 300 s. This was done to "reset" the surface of the carbon back to a stable poor wetting, so that changes in meniscus during normal polarization could be observed.

Two experiments were done with constant voltage, one with constant current. The values were chosen to ensure normal electrolysis conditions, without risking anode effect due to too quick depletion of the alumina content. The polarization voltages used were 3 V for the first run, then 6 A constant current for the second, and for the last experiment a polarization voltage of 4 V was used.

The weight change was observed by setting the starting weight to 0, and logging the weight change for the entire duration of polarization. Weight increase due to matter attaching itself on the anode rod, anode volume changes due to carbon consumption and reduction of liquid height due to evaporation was subtracted from the logged weight before it was presented.

4.5 Short anode effects

A test was conducted on a graphite cup anode to see how short anode effects affected the wetting of the anode surface.

First, the anode was preconditioned by polarizing at 3 V for several minutes at 20 mm. This was only done once, to ensure good wetting at the start of the experiment.

After this, the actual sequencing started. The lowest part of the anode was blocked by applying 25 V for 3 seconds in three different positions – first at 3 mm, then at 7 mm, and finally at 10 mm. It is necessary to do the block in steps due to limitations in the power supply. If too large areas are attempted blocked at once, the result is often that the power supply reaches its maximum current at a lower voltage, and hence normal electrolysis occurs. After retraction and reimmersion, the wetting at 10 mm and 20 mm was measured by stopping at these position during immersion and pausing for 1 minute.

Then the upper parts of the anode was blocked by applying 25 V for 3 seconds in three different positions – first at 13 mm, then at 17 mm, and finally at 20 mm. After retraction and reimmersion, the wetting at 10 mm and 20 mm was measured.

Then the lowest part was unblocked, by applying 3 V at 10 mm for 2 minutes before measuring wetting again. Finally, the upper parts were unblocked by applying 3 V at 20 mm for 1 minute. The entire sequence, excluding preconditioning, was repeated two times.

The sequence is summarized in Table 4.3.

Table 4.3: Sequence used for testing short anode effects

Step no.	Position relative to surface [mm]	Movement speed [mm/s]	Wait time [s]	Voltage [V]
1	-10	-	30	0
2 (recover)	10/20	0.2	120/60	3
2 (block)	3..7..10/13..17..20	0.2	3	25
3	-10	0.2	30	0
4	10	0.2	60	0
5	20	0.2	60	0
6	-10	0.2	30	0

After the last short anode effect, the anode surface was observed using an Hitachi TM3000 SEM.

4.6 Increasing anode effect time

The test on increasing anode effect time was conducted to check the decrease in wettability as a function of anode effect time. This test was conducted on a vertical graphite anode with a 30 mm tall carbon section.

The anode was first immersed to 21 mm (10 mm onto the carbon phase) and held there for 60 s to measure wettability. Then it was moved to 26 mm (15 mm onto the carbon phase) and held there for 60 s to measure wettability. After these 60 s, the anode was polarized. After polarization, it was held in the same position for 60 s before retraction.

For the first measurement, the anode was polarized for 60 s first at 3 V and then at 4 V, to ensure good wetting. For the subsequent measurements, 20 V was applied, inducing an anode effect. The duration of each polarization was increased for each dip so that the accumulated time of anode effect after the dips were: 1 s, 3 s, 5 s, 10 s, 30 s, 1 min, 3 min, 5 min, 10 min, 30 min, 60 min.

The sequence is summarized in Table 4.4.

Table 4.4: Sequence used for testing increased anode effect time

Step no.	Position relative to surface [mm]	Movement speed [mm/s]	Wait time [s]	Voltage [V]
1	-10	-	5	0
2	21	0.2	60	0
3	26	0.2	60	0
4	26	-	1/2/../1800	20
5	26	-	60	0
6	-10	0.2	5	0

4.7 Glassy carbon

A glassy carbon anode was tested, to see if the trends in wettability that were observed with graphite are also valid for other materials. The anode used here was the glassy carbon anode described in Section 3.2.4. The side of the crucible was shielded, to ensure that current only flowed out through the crucible bottom.

4.7.1 Voltage ramping 10 V to 1 V

For the first test, a voltage ramping was performed. The anode was held 10 mm above the melt, immersed 10 mm into the melt, held there for 120 s, polarized for 60 s and then held there for 180 s more before it was retracted. The starting voltage was 10 V, and the voltage was reduced in 1 V increments until 1 V. The entire procedure was repeated twice. The procedure is summarized in Table 4.5.

Table 4.5: Sequence used for voltage ramping of glassy carbon

Step no.	Position relative to surface [mm]	Movement speed [mm/s]	Wait time [s]	Voltage [V]
1	-10	-	30	0
2	10	0.2	120	0
3	10	-	60	10/9/../1
4	10	-	180	0
5	-10	0.2	30	0

4.7.2 Sectioning and stabilization

After the voltage ramping was finished, the anode was immersed 20 mm into the melt and polarized at 5 V for 120 s, before it was immersed to 10 mm and polarized at an anode effect inducing voltage of 10 V for 600 s. This was done to give one section with good wetting and one with poor wetting. This was done to enable observation of the different surfaces in SEM afterwards. Then the anode was immersed 15 mm into the melt and held there for 1200 s to observe the advancing wetting angle. The anode was immersed further into the melt and then retracted back to 15 mm with the same speed to observe the receeding wetting angle, and held there for another 1200 s. This was done to see if the anode is able to stabilize at the equilibrium wetting angle .

After this, the anode was taken out of the melt, and the surface was imaged using a Hitachi TM3000 SEM, to see if any structural changes had taken place.

4.8 Industrial anodes

Some of the experiments in the previous sections were repeated on vertical anodes with industrial carbon material (described in Section 3.2.5). The results from these experiments were compared to results from vertical anodes of graphite to see if the wetting behavior was similar. In some of the cases, SEM-images were obtained of the surfaces after polarization using a Hitachi TM3000 SEM.

4.8.1 Voltage rampings

A voltage ramping similar to the one conducted on the cup anodes in the reproducibility section was conducted. The anode was immersed 16 mm into the melt, meaning that the carbon was immersed 5 mm. It was held there for 120 s, then polarized for 60 s, and finally held for 180 s before it was taken out of the melt again. The voltage was increased in 1 V increments, starting from 1 V and ending at 10 V. The sequence is summarized in Table 4.6.

This was run on a vertical anode with 10 mm tall carbon surface and 22 mm diameter. The results for the industrial anodes were compared to results from testing on graphite anodes of identical shape.

A voltage ramping going from 10 V to 1 V was also conducted on two anodes. The procedures and anodes used are identical to the 1 V to 10 V ramping described above, with the only exception that the voltage was ramped downwards from 10 V to 1 V instead of upwards.

Table 4.6: Sequence used for voltage ramping on vertical anodes

Step no.	Position relative to surface [mm]	Movement speed [mm/s]	Wait time [s]	Voltage [V]
1	-10	-	30	0
2	16	0.2	120	0
3	16	-	60	1/2/../10
4	16	-	180	0
5	-10	0.2	30	0

4.8.2 Observing changing meniscus

The experimental procedure in this section is similar to the one in Section 4.4. An industrial anode with a 10 mm tall carbon surface was used. The anode was first run on a 120 s anode effect, to obtain stable poor wetting. After this it was underwent normal polarization for 300 s immersed to approximately the middle of the active carbon surface (16 mm immersed) before it was blocked again with a 120 s anode effect. Then the same polarization was repeated with the meniscus on the BN-phase (25 mm immersed). The results in the two cases were compared, in the same way as in Section 4.4.

The entire sequence was repeated three times, first at 4 V, then at 6 A and finally at 3 V. For the first 20 s of polarization, the voltage/current was slowly ramped up, to ensure that the anode would be able to pass current.

4.8.3 Increasing anode effect time

The procedure conducted here is identical to the procedure described in Section 4.6. An industrial anode with 30 mm tall active carbon surface was used.

Results and Discussion

To improve readability, the results and discussion has been merged into one section.

General behavior during wettability testing

As some readers may be unfamiliar with testing wettability on carbon anodes, a section on the general behavior has been included. This section outlines the resulting trends in weight vs. time and position when anodes are immersed into a cryolite melt and polarized, both at operating voltages and at anode effect inducing voltages. This is done to make it easier to understand the results discussed later on.

Cup anodes

The data from this section is taken from one of the polarizations in the reproducibility section. In both the cases shown, the anode has previously been polarized. Figures 5.1 and 5.2 illustrate the general weight change behavior for normal electrolysis (upper plots) and anode effects (lower plots). When the anode has the same characteristics over the entire surface, one obtains a smooth buoyancy corrected weight during immersion. However, as the current pull during polarization is not uniform over the anode, the resulting immersion/emersion curve for the sample is more uneven, as can be seen here in Figure 5.1. The immersion depth is somewhat less than 10 mm due to evaporation of the melt during the experiment.

During normal polarization, a sharp drop in weight occurs at the onset of polarization. This is due to bubble formation on the anode surface. The weight will then either stay constant during polarization or slowly creep higher as time passes. When the latter is observed, it is likely caused by convection. When polarization begins, the melt is not in motion, and the drag force on the created bubbles is small. This means that they can grow larger before detaching. When bubbles start detaching, this induces a stirring motion in the melt, and hence a larger drag force on the bubbles. This makes the bubbles drop off at an earlier point, and hence the weight slowly increases.

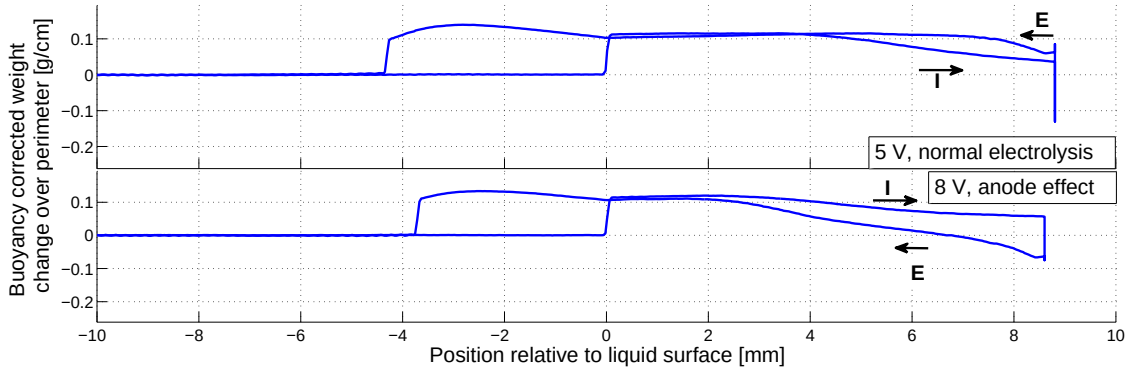

Figure 5.1: Buoyancy corrected weight change vs. position for a cup anode in a 1 wt% alumina melt. Polarization occurred for 60 s at bottom position. Upper plot shows polarization at 5 V, lower show polarization at 8 V, inducing an anode effect. I and E mark the direction of immersion and emersion respectively.

When an anode effect occurs, the wetting becomes poorer, and the weight drops. This can be seen in the lower plot of Figure 5.2. After polarization, the weight stays at approximately the same level.

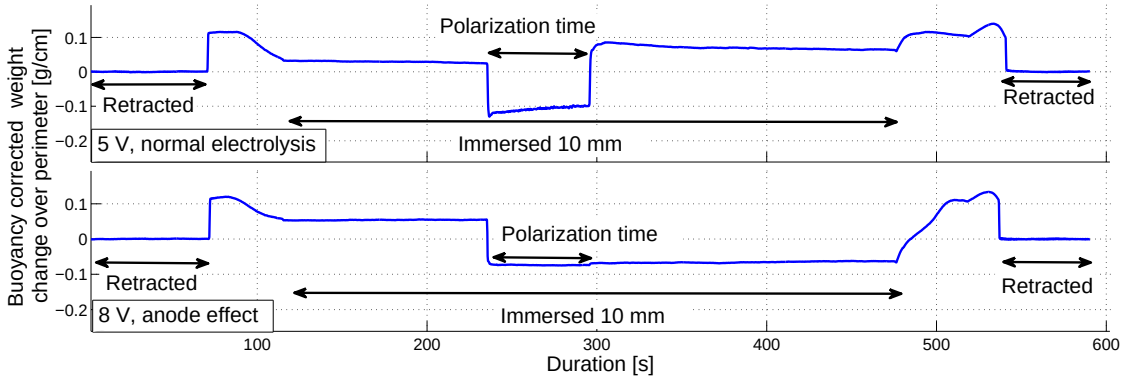

Figure 5.2: Buoyancy corrected weight change vs. time for a cup anode in a 1 wt% alumina melt. Polarization occurred for 60 s at bottom position. Upper plot shows polarization at 5 V, lower shows polarization at 8 V, inducing an anode effect.

Vertical anodes

The data for this section is taken from a vertical anode with a 10 mm tall active carbon surface and a diameter of 16 mm. The anode was polarized at various voltages both with the meniscus at the BN-phase and with the meniscus at the carbon-phase. In all the cases shown, the anode has previously been polarized at various voltages.

As the vertical anodes consist of several layers of material, the resulting buoyancy corrected weight is different for these materials than for a cup anode made solely of carbon. Figure 5.3 shows the buoyancy corrected weight change during immersion of a vertical anode with 10 mm active carbon area. The anode was immersed first over the 11 mm BN-section, then over 10 mm of active carbon, and then 7 mm up on the second BN-section. From the figure it is clear that the wettability of the boron nitride phase is good, with a wetting weight of around 0.1 g/cm, while the carbon phase has somewhat poorer wetting. As the BN-phase is not affected by polarization, the wettability will not change unless the electrolytic composition changes.

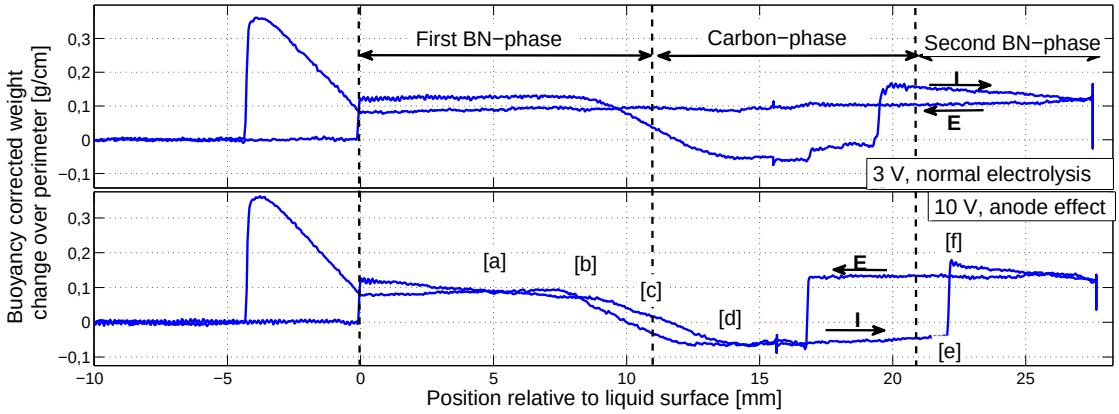

(a) Buoyancy corrected weight vs position relative to surface. Lables [a] to [f] corresponds to the six different stages shown in Figure 5.4

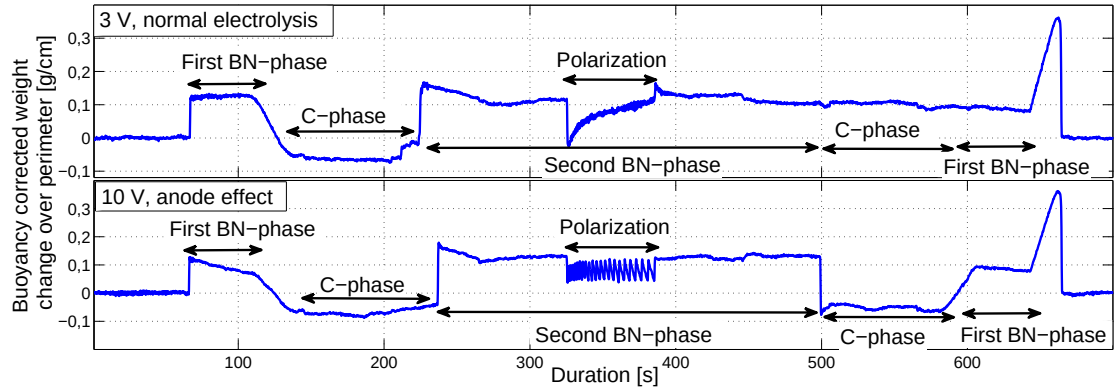

(b) Buoyancy corrected weight vs time.

Figure 5.3: Buoyancy corrected weight change for polarization at 3 V and 10 V on the BN-phase of a vertical anode with 10 mm active carbon. Polarization time of 60 s.

The theoretical movement of the meniscus during the immersion is sketched in Figure 5.4. In the sketches it is assumed that the wetting on BN is positive, and the wetting on carbon is negative. The first assumption is always true for this melt, the last one depends on previous polarizations, however it holds for both the cases in Figure 5.3. (a) shows the start of the immersion. As the wetting is positive, the meniscus is higher up on the

surface than the actual liquid level. In (b) the meniscus starts touching the carbon phase. As the wettability of this phase is poorer than the one of the BN-phase, the meniscus will no longer move upwards, but stay in place, while the immersion proceeds. This will cause a slow decrease in buoyancy corrected wetting weight during the transition (b)-(d). As the meniscus was higher up than the actual liquid level before the transition, and will end up at a level below the actual liquid level, this transition is expected to start some mm before the actual liquid surface is at the carbon-BN-interface and end some mm after. This is exactly the behavior shown in Figure 5.3a. As the anode gets further immersed, the new meniscus height for the carbon phase gets established (d), and the same wetting weight is kept until the meniscus reaches the second BN-phase (e). As the meniscus reaches the second transition, it goes from a phase that is poorly wetting to a phase that is well wetting. Here, one would expect a fairly immediate jump upwards in weight from (e) to (f) when the meniscus reaches the second phase, which is also observed.

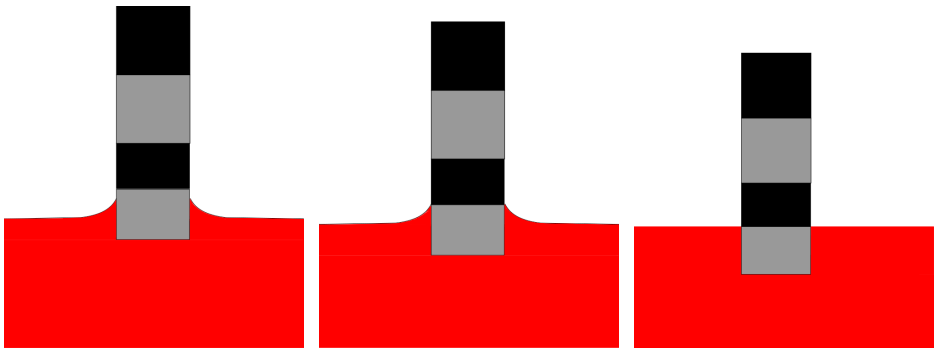

(a) Low on BN-phase (b) Start of first transition (c) During first transition

(d) End of first transition (e) Start of second transition (f) End second transition

Figure 5.4: Behavior of meniscus during immersion of a vertical anode into a cryolite melt. Grey area represents BN-phase, black represents carbon with poor wettability. As the melt wets carbon poorer than it wets BN, a gradual transition is observed when going from the BN-phase to the carbon-phase, while the opposite transition leads to an immediate jump in meniscus height.

It should however be noted, that this transition should happen at a liquid height higher than the height up to the second BN-phase – 21 mm. This is due to the meniscus bending

downwards on the carbon phase. This is observed in the 10 V immersion in Figure 5.3a, but for some reason the jump occurs earlier in the upper 3 V plot. It is unclear why this happens, but wave motion in the melt could possibly explain it. On the way out, the meniscus again moves through the stages (f) to (a). The only difference expected in the plot, is that the jump downwards at the first transition between BN and carbon occurs a lower liquid height, as the meniscus is higher up than the liquid level to begin with. This is also what is observed in the 10 V case.

Figure 5.5 shows the buoyancy corrected weight change when a vertical anode is polarized with the meniscus at the carbon phase. The anode was immersed first over 11 mm of BN-phase, and then 5 mm into the carbon-phase, before it was polarized. The anode has previously been polarized several times, suggesting that the wetting is already at its maximum level.

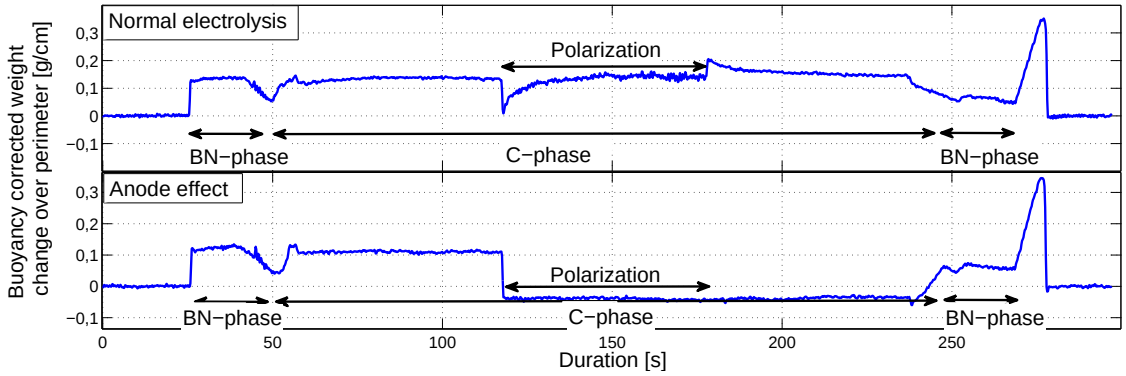

Figure 5.5: Buoyancy corrected weight change for 60 s of normal polarization (upper) and polarization causing AE (lower) on the carbon-phase of a vertical anode. In both cases the polarization voltage was 5 V, but in the second case the alumina content was lower.

When the polarization does not cause anode effect, the resulting weight drop during polarization is generally similar to the one observed when the anode was polarized with 3 V on the BN-phase, and is somewhat lower than what it is for polarization of the cup anodes. For the cup anodes, the drop was around 0.15 g/cm at the end of polarization, while this anode showed a drop of 0.12 g/cm in the beginning of the polarization, and less and less as the polarization went on. This is expected, as bubbles slide more easily off a vertical surface than a horizontal one.

An interesting change can be observed between the polarization on BN and the polarization on carbon, when anode effect occurs. For the 10 V polarization on BN (lower plot of Figure 5.3b), the weight appears to oscillate during polarization, while for polarization on carbon (lower plot of Figure 5.5), the behavior is the same as for the cup anodes, with a quick drop in weight at the onset of polarization, which then stays stable. The oscillations for the polarization on the BN-phase could be explained by CF_4-bubbles. Even during anode effect, some current is still running, and hence some gas is formed.

The current is somewhat higher when polarizing at BN, as the total area of immersed carbon is larger, however the effect is small. Hence the total gas production in these two cases should also be similar. As no weight change can be seen on the carbon phase during anode effect, it would suggest that the produced gas rolls off easily in small, undetectable bubbles. For the BN-phase, the gas appears to be stuck at some point, allowing larger bubbles to form before they detach. The likely point for these bubbles to get stuck on would be in the intersection between the carbon phase and BN-phase. If gas rolled freely off the carbon phase and then got stuck on the BN-phase until the bubbles reached some critical size, the above behavior could be explained. A possible explanation for this could be the following: During anode effect, CF_4 wets the carbon well, and has a small wetting angle. Hence, the bubbles are present as a thin layer covering much of the surface. BN is however unaffected by the anode effect, and hence still wets cryolite well, and CF_4 poorly. This means that the wetting angle of CF_4 will be much higher, and the bubble will grow into a rounder shape before moving further. The difference between the two cases is sketched in Figure 5.6.

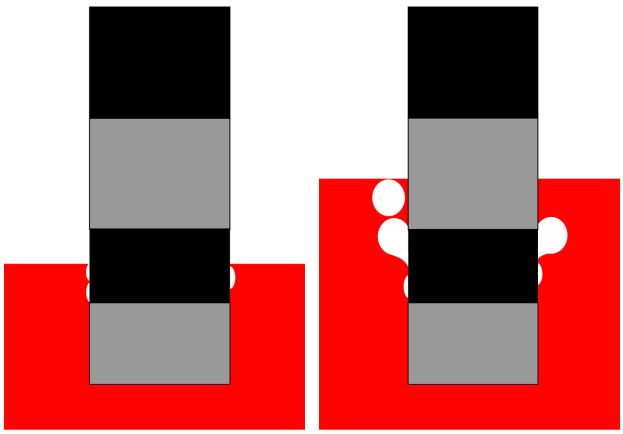

(a) Meniscus at C-phase (b) Meniscus at BN-phase

Figure 5.6: Sketch of difference in bubble release from anode effect on C-phase vs. on BN-phase of a vertical anode. Change in shape and size of bubbles are due to differences in wetting from the two materials. Bubbles can be seen as white shapes on the surface.

5.1 Investigating reproducibility

Having a good reproducibility is important. As high temperature experiments are both expensive and time consuming, there are limits to how many times an experiment can be repeated. Hence, it is important to be sure that realistic results are obtained from as few repeats as possible. To test how well results are reproduced, two tests were conducted. For the first part, the exact same experimental procedure was repeated for

three different anodes. If these three anodes obtain similar results, it is a good indication that the reproducibility of the method is good.

The second part of this section looks into how changing the experimental procedure affects the obtained results. Specifically it looks into whether the advancing and receeding wetting angles both move towards a common equilibrium angle, or if they stay different. If the latter is the case, it shows the importance of keeping this part of the experimental procedure as similar as possible for different tests, to ensure that the results can be compared.

5.1.1 Repeated procedure

When repeating the same procedure on three different anodes, the same general behavior was observed. Before any polarization, the wetting weights of the three anodes were fairly similar. After a few polarizations at low voltages, the weight change after removing and reimmersing the anode (green line in Figure 5.7) are still fairly similar, and the standard deviation can be seen to be low. At 7 V on the first ramping, all the anodes run into an anode effect, and the wettability quickly becomes poor. On the second ramping this occurs already at 6 V. The standard deviation for the wetting weight after reimmersion was 0.017 g/cm on average over all the polarizations. This is less than 8 % of the total allowed range for the weight measurements. The standard deviation after an anode effect was mostly lower than after normal electrolysis.

The measured wetting weight during and after polarization (blue and red line in Figure 5.7) can be seen to have a much higher standard deviation than the value after retraction and reimmersion (green). This is likely due to large variations in bubble formation on the anodes. During polarization, gas bubbles of CO/CO_2 are formed on the anodes, and will stay and grow on the anode surface until the drag force is sufficient to remove them. How large these bubbles grow depend both on the wettability of the surface (which in this case should be fairly similar for the different anodes) and on other factors such as geometry and tilting of the anodes. Zoric [34] reports that tilting a horizontal anode a fraction of a degree proved sufficient to induce significant buoyancy driven motion of gas bubbles. Such a small difference in tilt could easily happen for the anodes tested in this experiment, and would be very difficult to detect. Hence, one can assume that the larger standard deviation in weight during polarization is caused by some slight tilt. This could also cause the standard deviation after polarization, as some bubbles will still be attached to the surface. However, after retraction and reimmersion, the effect of bubbles on the surface should be removed, and hence only the weight change from wetting should be observed. As the standard deviation for this value is small, it suggests that the reproducibility of this method is good, and that approximately the same changes in wetting are observed for all the samples.

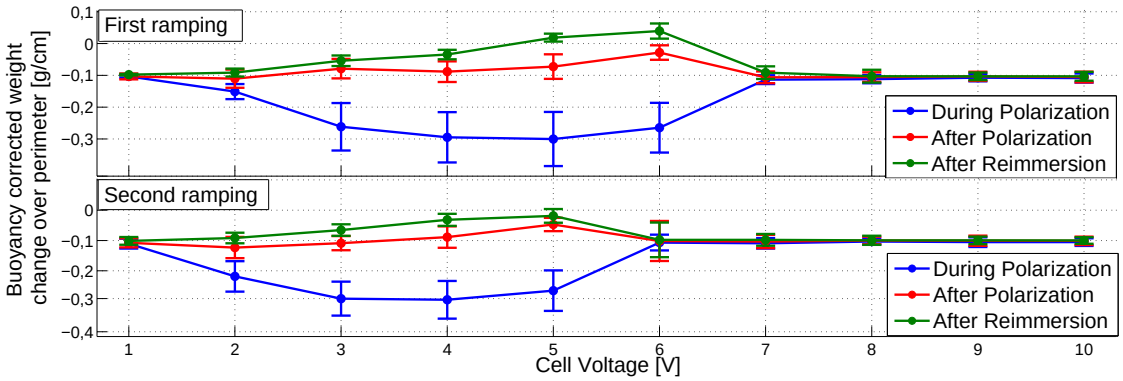

Figure 5.7: Wetting weights for polarization at different voltages for a 1 wt% alumina melt. Upper graph shows first voltage ramping, lower graph shows second. The values are an average over three different experiments. The error bars show one standard deviation in each direction.

5.1.2 Reaching equilibrium wettability

As was explained in the theory section, the apparent wettability may vary in a range between the advancing and receding value. This is due to surface heterogenity on a microscopic level, and due to dynamics in the system. When the system is kept still, the meniscus should slowly move towards the equilibrium value, however the time frame over which this movement takes place can be very large.

The results here show a large difference between the wettability obtained from immersing towards the set point and retracting towards it. In all the three different runs, the wettability found on retraction is much higher than the one found on immersion. This can be seen in Figure 5.8. The trends in immersion values are similar to the results in the previous section, with the wettability being low before polarization and after anode effect and somewhat higher after normal polarization. For the emersion values, the wettability is very high before polarization, somewhat lower after normal polarization and very low after anode effects. For the unpolarized anode, weight is translated into a wetting angle of 156^o during immersion, and 57^o during emersion. The value during immersion is corresponding best to other sources, which report wetting angles of 121^o and more for unpolarized carbon [1].

During the ten minutes logged here, both immersion- and emersion weights appear stable, and do not approach some common equilibrium value. This is worrying as it would imply that the result one gets for the wettability depends strongly on the experimental conditions. Even though, as was shown in the previous section, following the same experimental procedure yields very similar results, changing the experimental procedure will likely change the reported results. Hence, to compare results from different materials, it is important to keep the experimental procedures as similar as possible. Also, as the

observed weight changes greatly between the immersion value and emersion value, it is not possible to report equilibrium wetting angles from this method. Hence, the focus should rather be on observing the trends in wetting behavior.

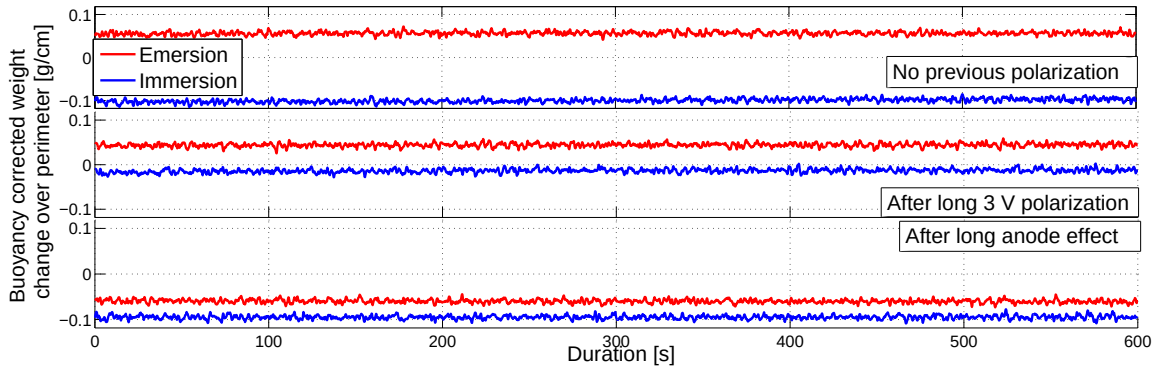

Figure 5.8: Measured weight change due to buoyancy at a position of 10 mm for an anode which has previously undergone no polarization (upper), long electrolysis (middle) or long anode effect (lower). Blue line shows wetting weight when the anode was advanced into the melt and stopped, red line shows wetting weight when the anode was retracted from further in the melt and then stopped.

5.2 Increasing alumina concentration

As mentioned in the theory section, there is general agreement that more alumina in the melt causes an improvement in wettability. However, many of these studies have been conducted using the Sessile Drop Method on unpolarized carbon. As it has been shown that polarization affects the wettability of the surface strongly, it would also be relevant to observe how varying the alumina content for a preconditioned anode affects the wetting. The anode was preconditioned with one part being poorly wetted, and the other being well wetted.

The experiment with feeding alumina showed almost no variations of wetting with changes in alumina concentration, as can be seen in Figure 5.9. Apart for the large difference going from 1 wt% to 2 wt%, the wetting weight in both parts of the anode remain approximately the same through all the alumina additions. The lower part of the anode, which had previously undergone normal electrolysis, appears to have an improvement in wetting at an alumina content of around 7 wt% and on, but the wettability is still much lower than at the start. At 11 and 12 wt% the wetting weight suddenly starts changing again, however at this point the melt is likely oversaturated, and undissolved alumina could be floating around the melt, disturbing the measurements. Not seeing an improvement in wetting after feeding alumina is surprising, as most sources report better wetting with higher alumina content [15]. Polarizing anodes in melts with higher

alumina content showed that the maximum wettability reached was better for these than for the 1 wt% melt (not shown in results). Hence, it is unlikely that the observed results are accurate.

The most curious thing about this result is how the effect of normal polarization and anode effect completely disappears when more alumina is added to the melt. Why the wettability suddenly drops is unclear, however it could possibly be linked to slow alumina dissolution. After alumina addition, the anode was held above the melt for approximately ten minutes before reimmersion. Studies on alumina dissolution [35, 36] suggest that this should be sufficient time for the oxide to dissolve, however in both these studies, the melt was stirred. As this was not done in this experiment, it is not unlikely that the alumina was not fully dissolved before measurements. This could cause a layer of alumina to be present at the melt surface, which would change the surface tension of the melt and hence its interaction with the anode. As it was not possible to include stirring in this set-up it is not possible to conclude whether this is the cause of the observed behavior.

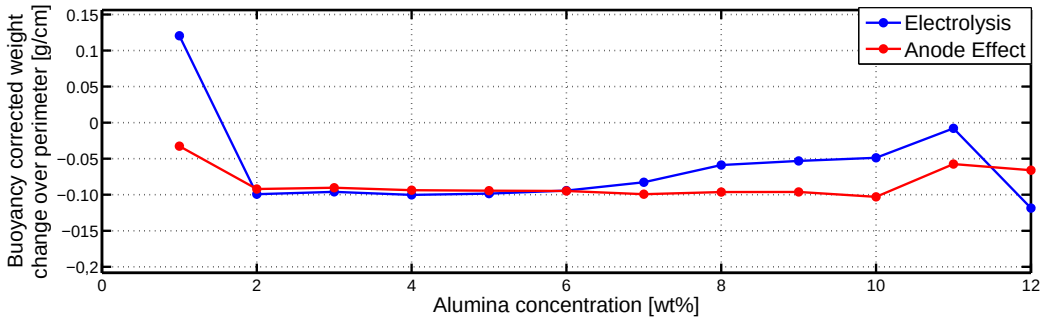

Figure 5.9: Buoyancy corrected weight change during alumina addition for two sections of a cup anode. The lower section (blue line) had undergone long electrolysis before the measurements, the upper section of the cup (red line) had undergone a long anode effect before measurements. Alumina was added in 1 wt% increments. The saturation limit is expected to be somewhat below 11 wt%.

As a side note, it should be noted that the buoyancy corrected weight of different melts can not be directly compared, as the weight is a function of both surface tension and wetting angle. However, the surface tension of the melt varies only a few percent over the entire range of alumina concentrations [15], and hence comparing only the weights should give a good indication of how the wetting quantitatively varies.

5.3 Bubble development on horizontal anodes

Anodes with only horizontal surface are ideal to observe bubble development on the anode surface. As the meniscus of the melt is located on boron nitride, which should be

unaffected by the polarization, one should not observe any weight changes from movement of the meniscus.

The observed bubble development showed a clear trend. At lower currents, development of a single large bubble on the surface is clearly observed. The weight drops slowly as the bubble grow larger, and then suddenly jumps back up again as the bubble is released. Then the weight is slowly reduced again by the buildup of another bubble. The same oscillations can also be seen in the voltage. The voltage increases during the bubble buildup as more of the anode surface is shielded then, and drops sharply when the bubble is released. This is shown in the upper plot of Figure 5.10.

At higher current densities, the frequency of bubble development is increased and the weight jump during release becomes smaller. When the current density becomes even higher, the frequency of the logger is no longer sufficient to observe single bubble release. This is shown in the middle plot of Figure 5.10.

At 2.5 A/cm^2, the anode runs into an anode effect, and the bubble detachment frequency is suddenly sharply reduced – often not a single positive weight jump is observed. The weight drops slowly and stably during polarization, reaching around 1.8 g weight reduction in the 60 s of polarization, suggesting that even at anode effect, the surface is still slowly being covered by. During the anode effects, the current density at the surface is around 0.1 A/cm^2. This effect is shown in the last plot of Figure 5.10.

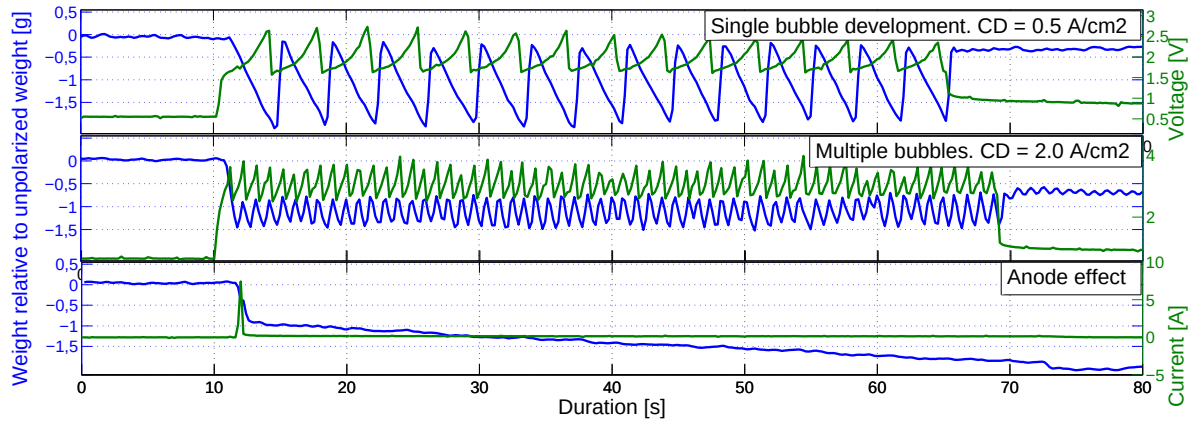

Figure 5.10: Weight and voltage/current (upper two/lower) response for different set current densities on an anode with only horizontal carbon surface. For the upper curve one can observe single bubble development, whereas the middle one has multiple bubbles forming at once. On the lower one, an anode effect occurs, apparently creating one large bubble that does not detach during the 60 s of polarization. The voltage during anode effect was stable at 20 V.

The trend in bubble size/detachment frequency is seen in Figure 5.11. As can be seen, the frequency of bubble detachment increases as the current density is increased. At the same time, the average weight change from bubble detachment is reduced, suggesting

that also the bubble size is reduced at higher voltages.

The weight decrease during bubble formation is lower than what one would expect if only CO_2 was produced and all the gas left the surface as one large bubble. For the lowest current densities, the weight drop is approximately 80 % of the expected value, for higher current densities it is even less. This suggests that not all bubbles on the surface grow into large ones before release. As the weight does not jump all the way back to 0 g after a bubble drop it is clear that some small bubbles are also present on the surface (see difference between middle and lower plot of Figure 5.11). It is possible that these could slide off before agglomerating into larger ones. If the bubbles are small enough, the weight increase from this process would be mostly masked by the weight decrease from formation of other bubbles. This effect appears to increase with increasing current density, however it is unclear whether this is an actual effect or if it is caused by limitations in the logging frequency. If this is an actual effect, it would mean that a larger fraction of the bubbles leave the surface as small bubbles at higher current densities. The maximum weight drop during polarization also decreases at higher current densities (last plot of Figure 5.11). This would imply either that the fraction of the surface covered by gas bubbles is reduced at higher polarizations, or that the thickness of the bubble layer is smaller at higher polarizations than it is at lower.

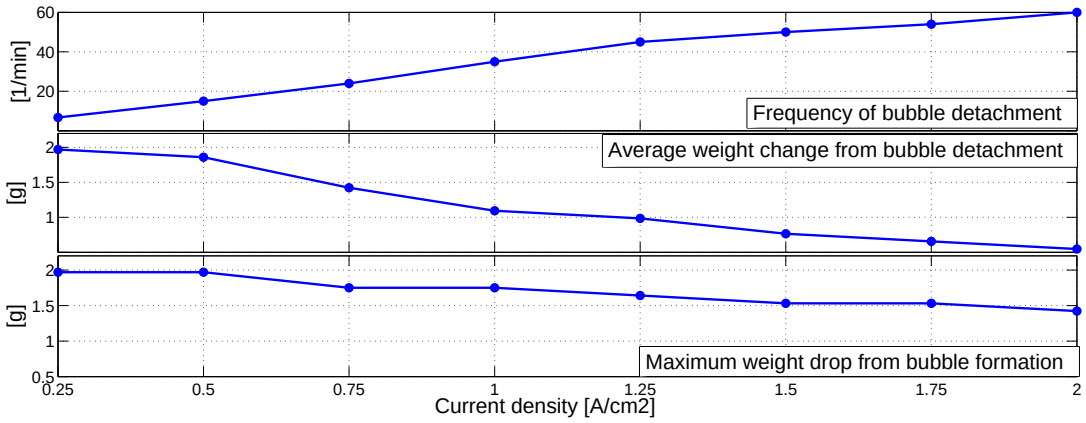

Figure 5.11: Bubble development on horizontal surface for current densities lower than the threshold for anode effect. Upper plot shows frequency of bubble detachment per one minute, middle show the average weight change from each bubble detachment and lowest shows the weight difference between the starting weight and the minimum weight during polarization. How these values are obtained is visualized in Figure 4.1 in the experimental section.

That the bubble coverage may in fact be reduced at higher polarization voltages and current densities has previously been observed by Zhao [21] for a 3.5 wt% alumina melt using a see-through-cell. Zhao observed that the average gas bubble coverage at the anode went from around 80 % to around 40 % when the current density was increased from 0.3

A/cm^2 to 1.3 A/cm^2. The following explanation was proposed: When the current density increases, the total gas production on the anode surface also increases, causing increased stirring of the bath. The increased stirring increases the drag force on the bubbles, and hence drags them off the surface earlier than before. However, changes in the wettability of the anode could also affect the bubble size. As has been shown previously with this apparatus [10], cryolite appears to wet the anode better at polarizations – as long as the voltage is not large enough to induce an anode effect. Hence, if the wetting towards the cryolite melt improves it would be easier to detach bubbles, and the same effect would be observed. A weakness of the experiment conducted here is that all the polarizations were tested sequentially on the same anode. Hence, the wetting of the anode has likely improved during the experiment. However, as the bubble size is not seen to grow smaller during one minute of polarization at a constant current density, the effect is likely small.

Having a smaller bubble coverage at higher current densities would be beneficial in industrial cells. Having a high current density is often more profitable as it will increase the current efficiency and allow more production per cell area. However, as the current density increases, the activation overvoltage on the anode will also increase, causing a higher voltage to be required to keep the reaction going [37]. This means that the energy consumption will increase. If at the same time the fraction of anode surface covered in bubbles also decreases, it would mean that the effective surface area increases. Hence the actual current density might not increase as much as the apparent one, and the increase in voltage would be smaller.

5.4 Observing movement of the meniscus

The advantage of the cup anode is that it yields a large perimeter length per volume of carbon immersed and hence a smaller error from buoyancy correction. However, due to the horizontal bottom surface, the bubble formation on these anode is usually fairly large. This means that it is difficult to measure changes in wettability during polarization, as the weight change due to bubbles being formed and rolling off gives the largest contribution to the weight change. By using a vertical anode, the bubble noise should be substantially reduced.

The idea of this experiment was to attempt to observe changes in the meniscus during polarization. Before each polarization, an anode effect was induced to reset the surface to stable, poor wetting. As boron nitride is insulating, and not participating in any reaction in the melt, the meniscus should not shift during polarization on BN. Hence, the only weight change observable on the boron nitride phase should be from bubbles. Thus, one expects that the weight during polarization on the boron nitride phase should first decrease due to bubble formation on the carbon phase, and then slowly increase again, as the amount of bubbles on the surface decreases. For the carbon phase, one expects the same change due to bubble formation (given that the currents are similar), but in addition, one would expect to see a increase in weight as the wettability improves,

and the meniscus moves upwards. Hence, this method should be suitable to determine how the wetting on the carbon phase changes during polarization.

For the first polarization at 3 V (Upper plot of Figure 5.12), the result is exactly as expected. For the carbon phase, a small drop is observed at first, and the weight is then slowly increased during the entire polarization, ending up at a value of around 0.15 g/cm higher than what it was before the polarization started. For the BN-phase, the drop at the start is much bigger, but after this, the same increase in weight is observed for this experiment as for the carbon phase. Based on this, it seems that polarization at lower voltages have a positive effect on the wetting of carbon already during polarization. As the drop in weight at the start of polarization is so much smaller for the carbon phase than for the BN-phase, it would also suggest that some improvement of the wetting happens almost immediately after the voltage is applied.

The two other graphs (middle and lower of Figure 5.12) however, show a somewhat different trend. Though the polarizations on BN in both cases look similar, they both end up at a higher value than before the polarization, suggesting that the meniscus is now shifted higher than it was before polarization. After retraction and reimmersion however, the previous value is retained, suggesting that no actual change in wettability has occurred on the BN-phase. The weight change at the carbon phase during polarization is also different for these runs. The drop at the start of polarization is still small, but after around 2 minutes of polarization, the curve starts being jagged, with sudden drops downwards. The cause of these drops is not clear. It could of course be formation of a large bubble, that is not rolling off as smoothly as the others, but as it can be seen in Section 5.3, bubble formation usually happens more slowly, with a slanted weight reduction during build up, and a quick increase during release. Although the total current here is higher than for the experiment with the horizontal anode, it is still unlikely that weight change due to bubble formation would take that shape. The other possibility would be that the meniscus suddenly jumped downwards, however why this would happen is difficult to imagine. The current/voltage jumps at the same time as the weight drops (not shown in the figures), which proves that the weight drop really is connected to the meniscus, and not simply caused by for instance matter falling off the rod as the experiment progresses.

The weight increase at the BN-phase could possibly be explained. As was seen in Figure 5.8 in the reproducibility section, the height that the meniscus stabilizes at is not necessarily the equilibrium value, but is related to the experimental procedure. By varying between immersing and emersing, vastly different wetting values were obtained. Although the anode in this case is kept in position, the bubbles formed on the anode will roll up the side of the anode until it is released. It is not impossible that such a process could shift the meniscus to a new position on the surface, where it would subsequently stay. Hence, one would observe a change in the wetting weight even though no change has actually taken place on the anode surface.

Though this effect could also take place at the carbon phase, the fact that the weight during polarization is higher for polarization on carbon for all three cases, even when

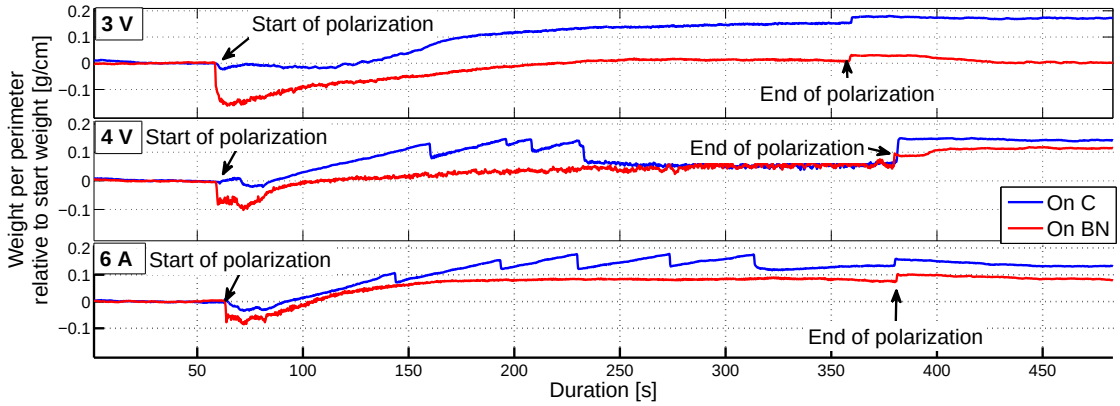

Figure 5.12: Weight change during polarization for polarization on carbon phase (blue curve) and boron nitride phase (red curve) of a vertical anode with 7 mm graphite height. Current during 3 V polarization was 4 A for polarization on carbon and 4.5 A on BN, during 4 V it was 5.8 A and 7 A respectively.

the current is similar, would still suggest that the wetting on carbon is improved already during polarization. Although these experiments do not give any information as to why the wettability is improving, it seems plausible that the changes in wettability could be caused by some adsorption or bonding reaction of the surface. As the wettability can improve much beyond the wettability for an unpolarized anode, removal of CF-bonds created during anode effect is not a sufficient explanation for the observed behavior. The improvement in wettability could be imagined to either stem from adsorption of gaseous species on the surface, or from creating of strong bonds between the carbon surface and some other specie (for instance O).

Showing that the improvement in wettability happens while the anode is being polarized is important. Though it is clear from previous results that polarization at lower voltages improves the wetting, this improvement could in theory stem from reactions happening after the voltage has been turned off. As any interruptions in current flow in an actual industrial electrolysis cell is unwanted and rarely happens, understanding the changes in wettability during polarization is more relevant for industrial purposes.

5.5 Short anode effects

Short anode effects were studied to get a better understanding of what causes the anode to become dewetting during anode effect. It has previously been observed that the surface of the anode becomes smoothly polished during long anode effects (shown in Figure 2.6b), however it is not clear if the surface polishing has any effect on the wettability. By inducing anode effects lasting only a few seconds, it is hoped that one will be able to have an anode effect that does not affect the topography of the anode. If this still results

in a decrease in wettability, it would imply that surface polishing is not the main cause of poor wettability after anode effects.

The results from the short anode effects showed an interesting trend. First of all, even short anode effects result in reduced wetting. In this case, the short block usually resulted in a wetting weight of around -0.12 g/cm, as can be seen in Figure 5.13. This is comparable to the wetting weight observed from the 60 s anode effects tested in the reproducibility section (Figure 5.7), which were around -0.10 g/cm. This would suggest that the surface changes causing poor wetting during anode effects happen very quickly.

A more curious effect is that when blocking occurs at 20 mm, the anode surface at 10 mm actually appears to improve. The wetting is in most cases still poor, but even so better than what it was after the anode effect at 10 mm. The opposite effect appears to be present during the recovery. When normal electrolysis occurs at the surface up to 20 mm, the wetting on 10 mm is actually worse than what it was before this electrolysis took place. If one simply reimmerses the anode without any polarization, no changes in wetting are observed, suggesting that the change in wetting must come from the subsequent polarization, and not simply from a change in wettability over time.

The improvement in wetting from a subsequent anode effect further up on the anode can be partly understood. When the anode is immersed to 20 mm to be blocked there, only the part between 0 and 10 mm is already blocked, the section between 10 and 20 mm still has good wetting until the new anode effect occurs. Hence, for a very short time before the anode effect is able to block the surface, one would expect a large current spike. This might be sufficient to partly unblock the surface up to 10 mm. As the results in Section 5.4 suggest that improved wettability may happen very quickly, it would be possible that the surface now is better wetting than before. After this, the anode effect will again cause the surface to wet poorly, but as more surface is now available, the new blocking might not reduce wettability to the same extent. Hence an apparent improvement in the wetting of the section up to 10 mm is observed.

That the wetting at 10 mm becomes worse when 3 V is applied at 20 mm is more surprising. The observed wetting weight of around -0.04 - -0.02 g/cm is hardly a very high wetting weight, and one would expect that higher values would be possible. Values of almost 0.05 g/cm were observed during the first voltage ramping in the reproducibility section (Figure 5.7). As the wetting usually improves for every polarization until a maximum value is obtained [10], one would expect that polarization at 20 mm would improve the wetting at 10 mm, not diminish it.

After the last short blocks, the anode was removed from the melt and its surface was observed using a SEM. The images obtained are shown in Figure 5.14. As can be seen, the anode surface after short anode effects looks similar to the surface after normal electrolysis. Hence, it would appear that changes to the topography of the sample is a result of the anode effect, and not a cause of the diminished wettability observed. This would be in agreement with the claims of Haverkamp [31, 32] that the reduction in wetting could be caused by formation of CF-bonds on the anode surface.

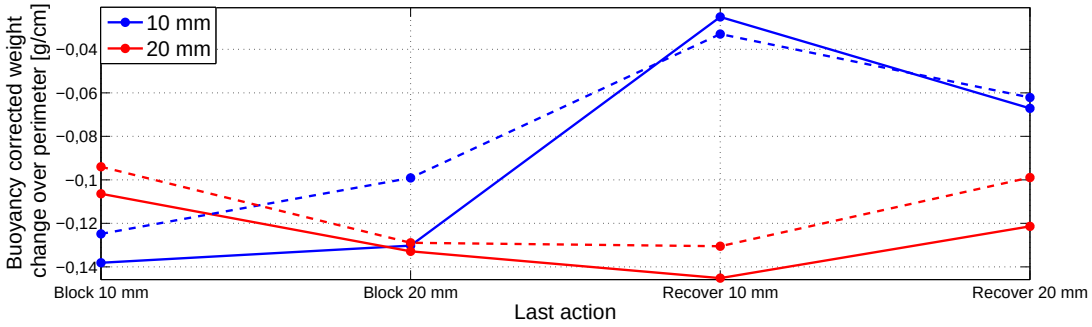

Figure 5.13: Buoyancy corrected weight change after reimmersion at 10 mm and 20 mm of a cup sample after inducing anode effects (3 s on 25 V) and recovering surface (2 min on 3 V for 10 mm / 1 min on 3 V for 20 mm. Solid line = 1st run, dashed = 2nd run.)

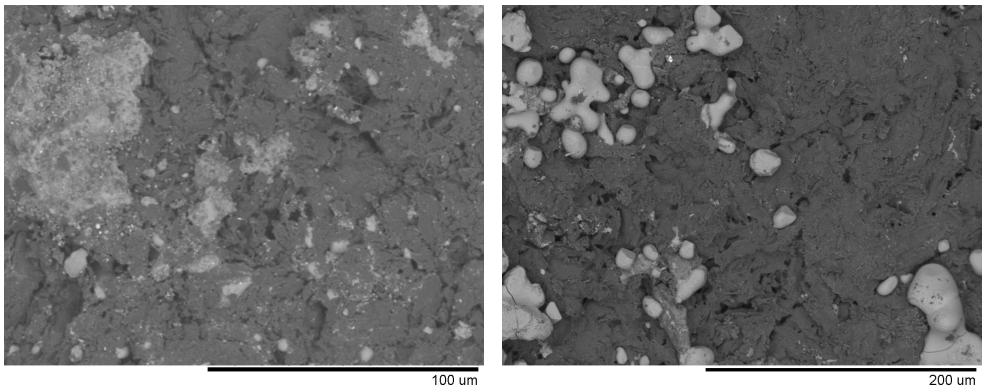

(a) After short anode effect (b) After normal electrolysis. From [10].

Figure 5.14: SEM images of surface of a graphite carbon anode after a few seconds of anode effect compared to surface after normal electrolysis shown in [10].

5.6 Increasing anode effect time

The previous section shows that also very short periods of anode effect have large effects on the wettability of the anode, and that wettability is not necessarily linked too strongly to the surface polish of the anode. It is however still possible that polishing the surface from longer anode effects may diminish the wettability even further.

In this part, the wetting of an anode which undergoes longer and longer anode effects is tested. As can be seen in Figure 5.15, the wetting drops fairly sharply during the first few seconds of an anode effect, but then levels off at a stable value. The same trend is observed in the position where the meniscus was placed during anode effect (red line) and the position that was immersed 5 mm during the anode effect (blue line). Already after 10 s, most of the reduction in wettability is obtained, and after 60 s, no extra

reduction in wettability is observed. As most of the reduction in wetting weight occurs before substantial surface polishing has had time to occur, this again shows that the geometric structure of the surface on a micrometer scale has little effect on the obtained wettability.

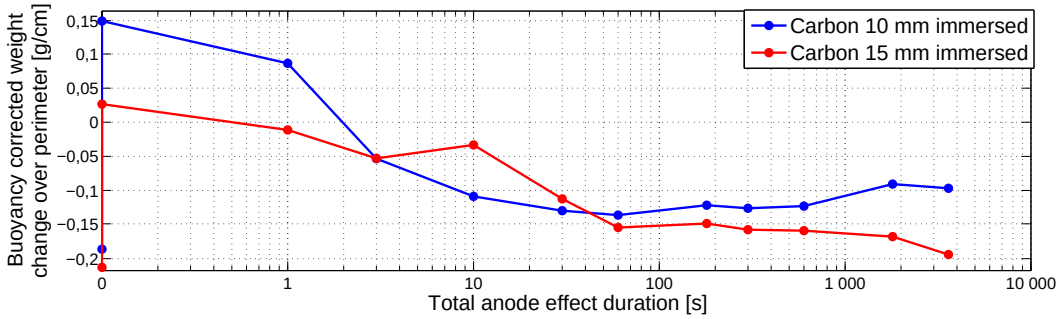

Figure 5.15: Calculated wetting weight on two positions on the carbon surface of a vertical anode after anode effects of various duration. The two points at 0 s represents value for an unpolarized anode (lower) and for the surface after preconditioning (upper).

5.7 Glassy carbon

Testing with glassy carbon was done to see how changing the anode material would affect the results. Both of the anode types are carbon based, however the structure is vastly different, and hence also the wetting behavior would likely be different.

Unpolarized glassy carbon was shown to be fairly poorly wetting, with a buoyancy corrected weight of around -0.08 g/cm . The curve for immersion and emersion is shown in Figure 5.16. This value is slightly better than the wetting weight of -0.10 g/cm obtained for graphite.

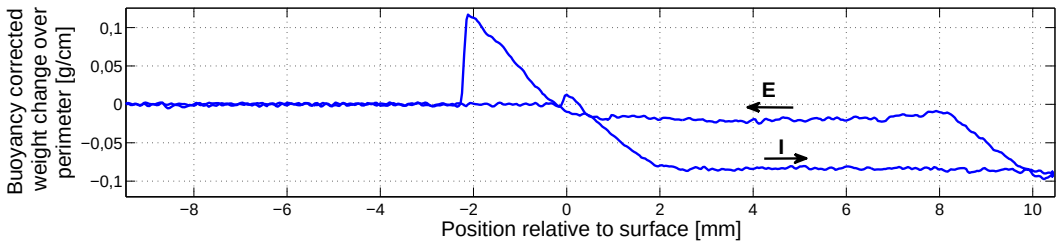

Figure 5.16: Buoyancy corrected weight change for immersion of a glassy carbon anode 10 mm into a 1 wt% alumina melt.

5.7.1 Voltage ramping 10 V to 1 V

During polarization, glassy carbon showed itself to behave very differently from normal graphite, by being considerably more resistant to anode effects than the normal graphite anodes used. The voltage rampings for the glassy carbon anode is shown as the solid lines in Figure 5.17. For the first voltage ramping from 10 V to 1 V, it went through the entire series without blocking, and for the second ramping it only blocked at 10 V and 9 V. For comparison, ramping from 10 V to 1 V on a cup anode was done in [10]. There the anode did not go out of anode effect until 5 V on the first run, and 6 V on the second run. The anode used in [10] is mostly poorly wetted during the entire first voltage ramping, but improves wettability at the last parts of the second ramping. These values are shown as the dashed lines in the figure.

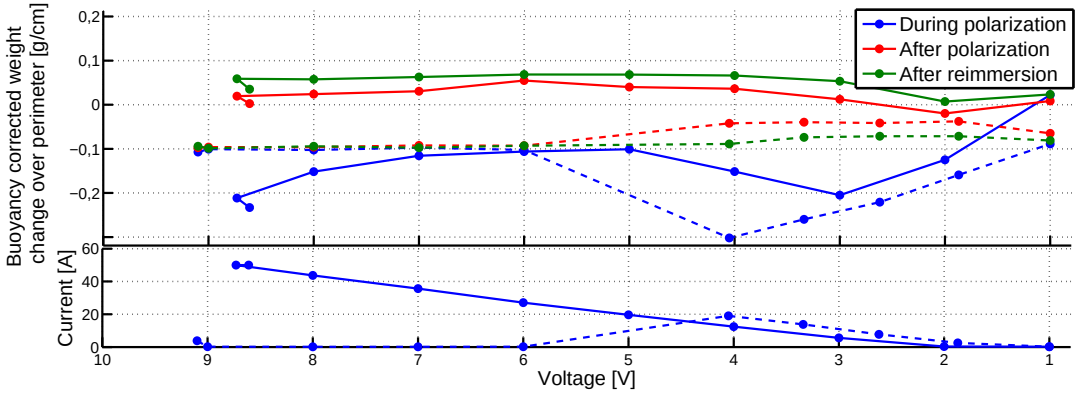

(a) First voltage ramping

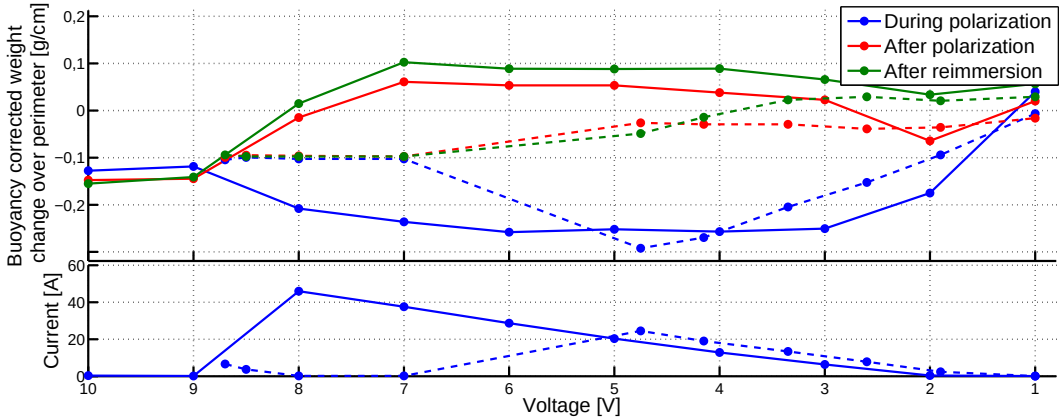

(b) Second voltage ramping

Figure 5.17: Buoyancy corrected weight change and currents for voltage ramping from 10 V to 1 V for a glassy carbon sample compared to a graphite cup anode tested in [10]. Solid line are values for glassy carbon, dashed line are the values for the graphite cup anode.

Though unpolarized glassy carbon is fairly poorly wetted, the anode very quickly becomes well wetted when it is polarized. In fact, the anode stabilized at a wettability after reimmersion of around 0.05 g/cm already after the first polarization, and stayed at approximately the same level for the entire first voltage ramping. On the second ramping, anode effect occurs at 10 V and 9 V, causing the wetting weight to drop down to around -0.12 to -0.14 g/cm. However, the surface again quickly recovers after the anode effect, and already after two more polarizations, the wetting is back to a high value again.

The weight change during polarization showed some mostly the same effects as for the graphite anodes. Figure 5.18 shows the plot of buoyancy corrected weight vs. time for when the anode is immersed 10 mm into the melt. First it is held there for 120 s, then polarized for 60 s, and then held there for 180 s more. The upper plot, showing the anode effect at 10 V shows a result very similar to what is observed for the graphite cup anodes – the weight drops sharply at the start of polarization, and then stays at that value both during and after the polarization.

The polarization at 5 V shows the same trend as for the graphite anodes. The weight drops sharply at the start of polarization, and jumps equally sharply up after the polarization is done. The weight is somewhat lower after the polarization than before, likely due to bubbles being formed on the anode surface. The lower polarization shows another curious trend. At 1 V there is nearly no current passing through the anode, and still one observes an increase in wetting during polarization. The exact same trend is observed in both of the polarizations at 1 V. This could imply that the polarization itself has a temporary positive effect on the wetting, which causes the meniscus to slowly creep upwards during polarization. However, it could also simply be that the effect is caused by electrostatic effects and are completely unrelated to wettability.

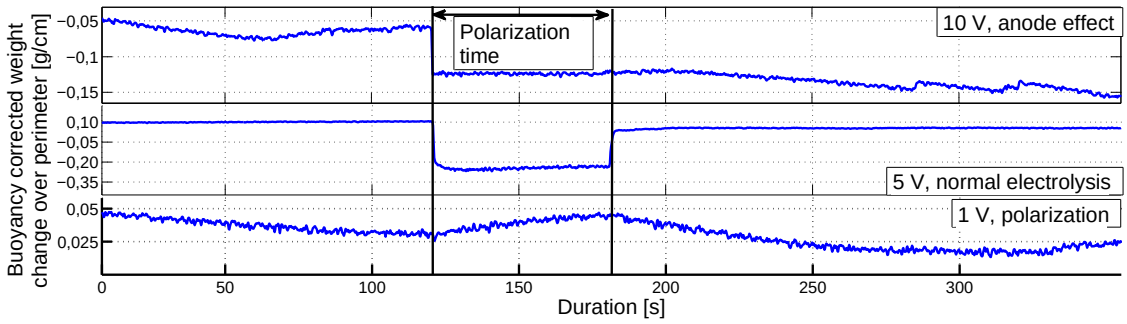

Figure 5.18: Buoyancy corrected weight change for polarization of glassy carbon sample at 10 mm immersion depth. Anode is kept at the same position during the entire duration. Solid black lines indicate the period in which the sample was polarized. The polarization voltage was 10 V for the uppermost 5 V for the middle one and 1 V for the last.

5.7.2 Sectioning and stabilizing

The anode was sectioned, to see if one could observe a difference between the anode surface after normal polarization and after extended anode effect. The glassy carbon anode, contrary to the graphite anodes previously observed (Figure 2.6), showed very little difference between the surface after anode effect, after normal electrolysis and before any polarization. The SEM-images obtained in the three cases can be seen in Figure 5.19. In all the images, the anode surface appears smooth, with only a few pores in them. Hence, despite the three surfaces having a vastly different wettability, the geometric structure of them appears equal on the micrometer scale. This means that whatever is making these surfaces wet differently, it must have another explanation than only structural change. Again, looking into the reasoning of Haverkamp [31, 32] would be relevant. In the articles it is observed that CF-bonds are formed before anode effect is initiated, and it is argued that the formation of these bonds may result in a changing surface tension. This could again lead to the surface wetting poorer. Similarly, one can imaging creation of other bonds during normal electrolysis. Detecting these bonds with the methods used in this project is however not possible.

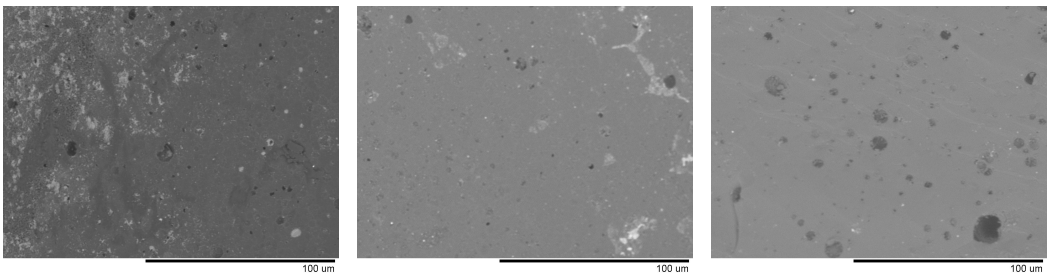

(a) Long anode effect (b) Normal electrolysis (c) Internal part, unpolarized

Figure 5.19: SEM images of surface of glassy carbon. Scale bar is 100 μm.

As the surface of the glassy carbon anode is fairly smooth, effect of hysteresis should be smaller than for the rougher graphite anodes. Hence, one would expect the a smaller difference in advancing and receding wetting angle.

The results resulting wettability obtained from immersing towards the set point and retracting towards it for the glassy carbon anode is shown in Figure 5.20. As can be seen here, the weight during immersion is actually increasing more than 0.025 g/cm over the 1200 s that has been logged here. Although the value is still far away from the value obtained when the anode is stopped while being retracted, the movement of the meniscus is still visible, and it is possible that the two wetting weights would eventually have become similar, had the anode been immersed for an even longer time. For comparison, the graphite cup anode observed in Figure 5.8 had a stable weight through the 600 s it was observed both on immersion and emersion. Also in this case, difference in wettability between the advancing and receding case was around 0.05 g/cm.

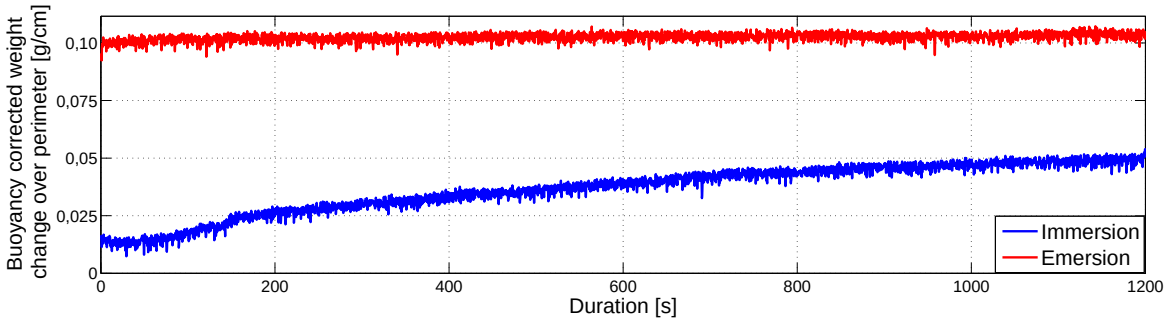

Figure 5.20: Measurements of buoyancy corrected weight change for glassy carbon anode after normal electrolysis. Blue line shows the weight when the anode was immersed and then held in position (advancing), red line shows the weight when the anode was retracted to this position and then held there (retracting). In both cases, the wait time on each stop was 1200 s.

The observed movement of the meniscus could be related to the surface structure of the anode. While the glassy carbon anode has a rather smooth surface, the graphite anode is usually only smooth after extended anode effect, and is observed to be more rugged after normal electrolysis (See Figure 2.6). It would likely be more difficult for the meniscus to move on the normal graphite than on the glassy carbon, as the actual wetting angle would be constantly changing (sketched in Figure 2.2). As the glassy carbon anode is fairly smooth, one would expect the meniscus to slide more easily over this surface, and hence it should be easier to move to an equilibrium wetting weight. However, even after a 20 minute wait, the advancing and receding wetting weights are still very difference. This means that the transition towards equilibrium is still too slow to make observations of the equilibrium angle feasible in these experiments. Hence, it would seem that one must settle for standardizing the experimental procedure and reporting relative changes to wettability instead of reporting equilibrium wetting angles at each stage.

5.8 Industrial anodes

Testing wetting on graphite anodes shows clear trends in wetting behavior. The advantage of using graphite is that it is easily accessible, easy to process and the reproducibility appears to be fairly high. However, graphite is not used in industrial settings, and hence it is necessary to test if the observed behavior is similar for anodes made of coke and pitch. To do this, some of the experiments conducted on graphite anodes were repeated on sample industrial anodes. The anodes used in these experiments are described in Section 3.2.5.

5.8.1 Voltage rampings

The general trends from the voltage rampings is that the industrial anodes have a very similar behavior to the graphite ones. They pull approximately the same current, go into and out of anode effect at approximately the same voltages, and have a generally similar wetting weight. The wetting weight during the two rampings can be seen in Figure 5.21. For the ramping from 1 V to 10 V, the industrial anode runs normal electrolysis until 6 V, while the graphite anode only runs electrolysis until 5 V. On the other hand, the graphite cup anodes tested in the reproducibility section were also able to run electrolysis until 6 V, and hence the early anode effect from the vertical graphite anode could simply be coincidental.

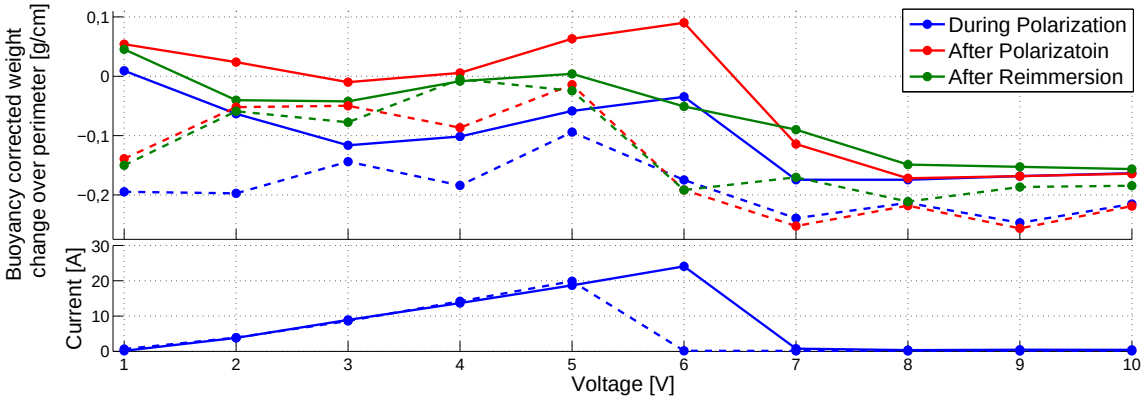

(a) Voltage ramping 1 V to 10 V

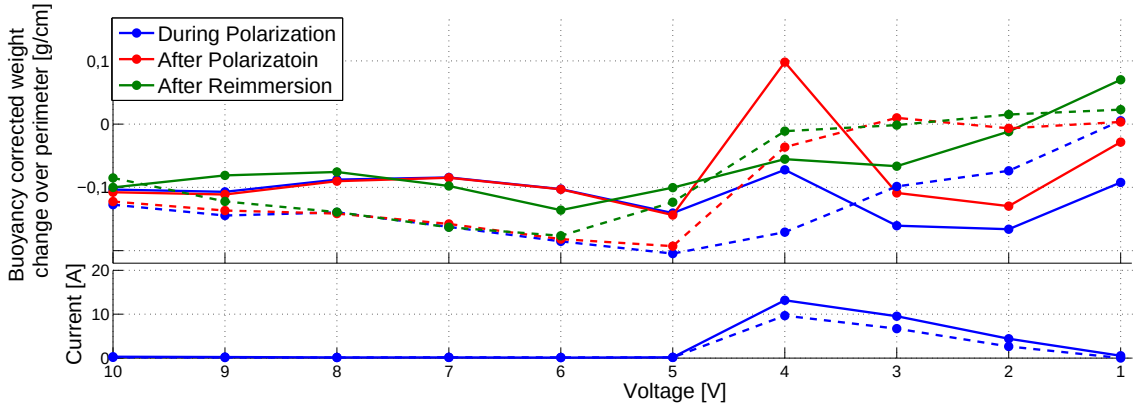

(b) Voltage ramping 10 V to 1 V

Figure 5.21: Comparison of two identical procedures for voltage ramping from 1 V to 10 V, and from 10 V to 1 V for industrial (solid line) and graphite (dashed line) vertical anodes. The only difference between the two anode designs was the material used for the carbon part.

In both of the rampings, the industrial anode appears to have a marginally better wetting after anode effect has been induced, however the variations are not too large. During normal electrolysis, the wetting after reimmersion is fairly similar between the two, especially during the ramping from 1 V to 10 V.

5.8.2 Observing changing meniscus

Also here, the industrial anode appears to behave similar to the graphite anode observed in Section 5.4. In all the three cases shown in Figure 5.22, polarizing at the carbon phase yields a quick weight drop in the beginning, followed by a slow increase in weight as the polarization time increases. In all three cases, the weight increases more while polarizing at the carbon phase than it does at the BN-phase, suggesting that the meniscus on the carbon-phase is slowly moving upwards. This was the same general behavior that was observed for the graphite anodes in Section 5.4, except for the fact that the strange jumps in the curve were not observed with the industrial anodes.

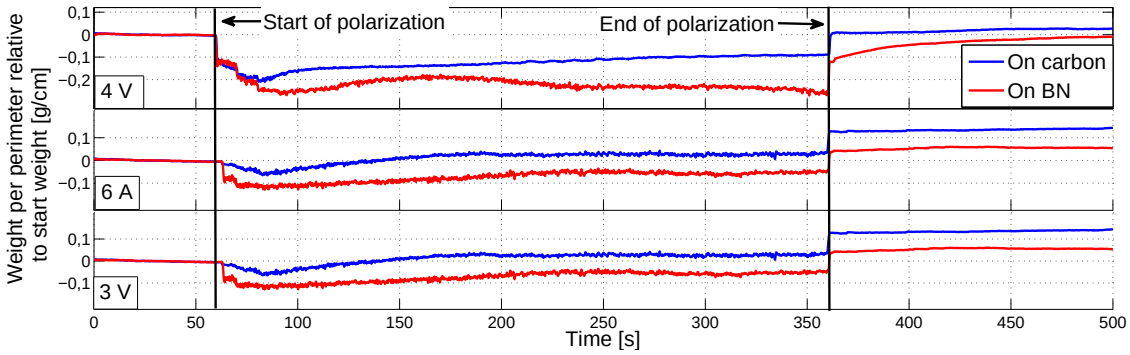

Figure 5.22: Weight change during polarization for polarization on carbon phase (blue curve) and boron nitride phase (red curve) of a vertical industrial anode with a 10 mm tall active carbon surface. During the 4 V-polarization, the current was 10-11 A for polarization on the carbon phase and 18-19 A on BN. For the 3 V-polarization it was 8 A and 10 A respectively.

5.8.3 Increasing anode effect time

The industrial anode showed a behavior very similar to the behavior of the graphite anode. The reduction in wettability with increased anode effect time is shown in Figure 5.23. The anode responds well to the 120 s preconditioning, and obtains a positive wetting after this. In comparison to the graphite anode, the wetting before any polarization is somewhat better, but after the preconditioning, the wettability of the two anodes were similar. The industrial anode had a faster decrease in wettability after anode effects, needing only a second to go to the poorest wetting. In comparison, the graphite anode

needed around 10 s to reach a stable weight after anode effects. The industrial anode levels off at a wetting weight of around -0.1 g/cm after long anode effects, while the graphite anode decreased to a somewhat lower level.

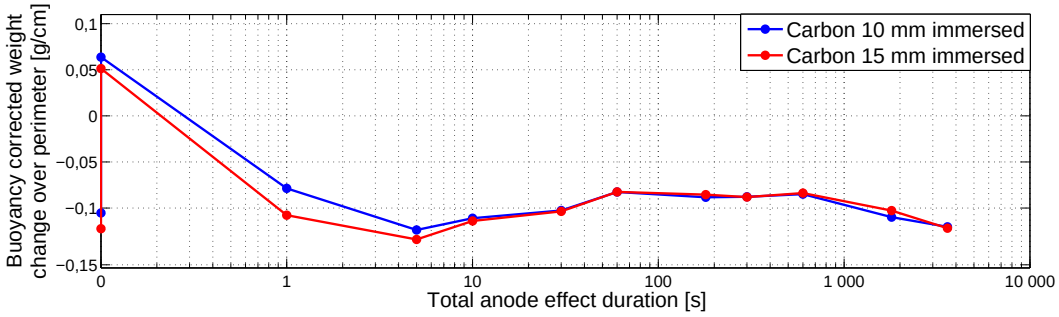

Figure 5.23: Calculated wetting weight on two positions on the carbon surface of a vertical industrial anode after anode effects of various lengths. The two points at 0 s represents value for an unpolarized anode (lower) and for the surface after preconditioning (upper).

5.8.4 Comparing surface structure of graphite and industrial anodes

There is a large difference in the surface structure of the graphite and industrial anodes. The difference in structure after some polarization can be seen in Figure 5.24. The graphite, consisting of only one material is fairly smooth and uniform over the surface, also at the micrometer-scale. The industrial anodes on the other hand, consisting of single source coke grains with a pitch binder, are much rougher. If one zooms in more, scales and pores can be observed in the structure. In addition, the industrial anode appears to be covered by a layer of cryolite.

Even though cryolite wets both surfaces well and roughly even after electrolysis, the layer of cryolite is only observed for the industrial anode. This is likely caused by the rougher structure of the industrial anode. With the fairly flat, nonporous structure of the graphite anode, there are few places for the melt to stick onto when the anode is retracted, and hence the melt can slide off more easily. The industrial anode provides more cavities in the surface which can better hold onto the cryolite, and hence more cryolite is observed to stay on the surface in this case.

As previously mentioned, the surface of graphite anodes become very smooth after extended anode effects. The same effect is present for industrial anodes, however the effect is less pronounced. As can be seen in Figure 5.25, the anode surface is mostly smooth also for the industrial anode, but several areas still retain some roughness. When zooming into these areas, a somewhat porous structure can be observed, with pores likely running

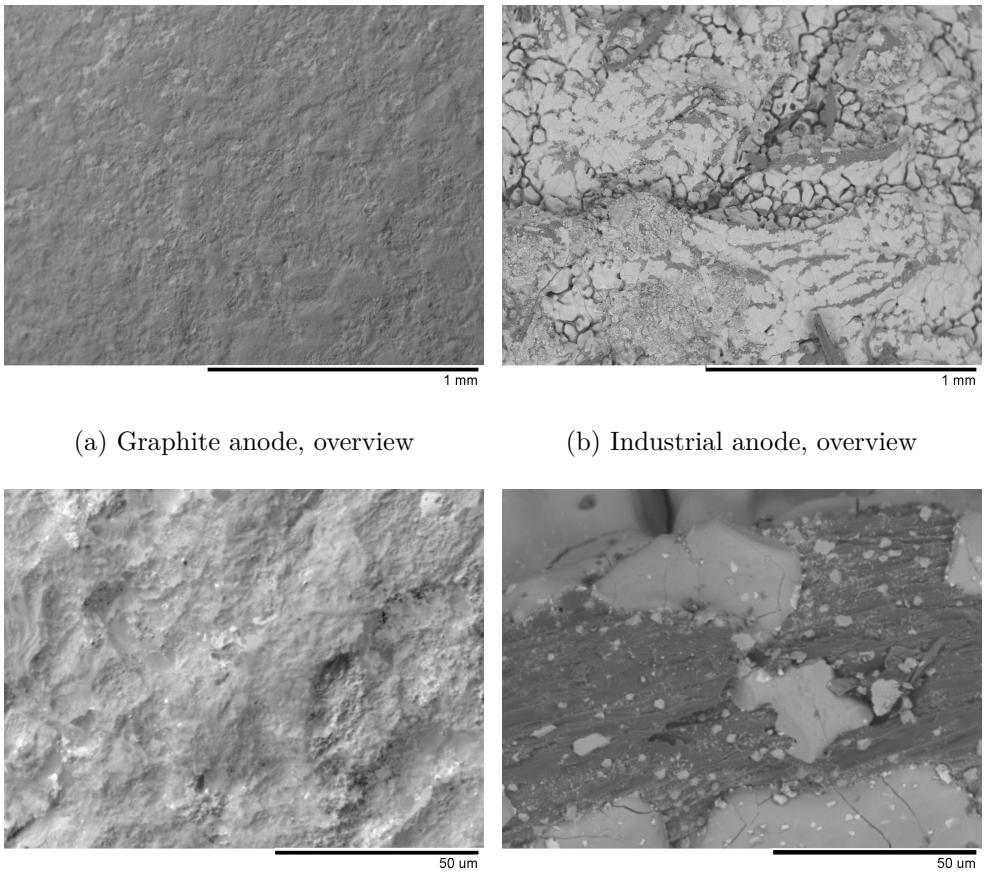

(a) Graphite anode, overview

(b) Industrial anode, overview

(c) Graphite anode, zoomed

(d) Industrial anode, zoomed

Figure 5.24: SEM images of surface of graphite and industrial vertical anodes after electrolysis.

deep into the anode. These pores were likely also present after normal electrolysis, but would have been difficult to detect due to the layer of cryolite that was observed on the surface in Figure 5.24. After extensive anode effects, cryolite was no longer present on the surface after the anode had been removed and cooled down. This is hardly surprising, as the anode after this was wetting the cryolite much worse than before.

In summary one can say that the general wetting behavior of the industrial anodes appear to be similar to the graphite anodes. However, as the industrial anodes consist of several components and different grain sizes, one can expect a larger difference in behavior between different anodes, and the reproducibility of testing on industrial anodes is likely somewhat lower than for graphite ones.

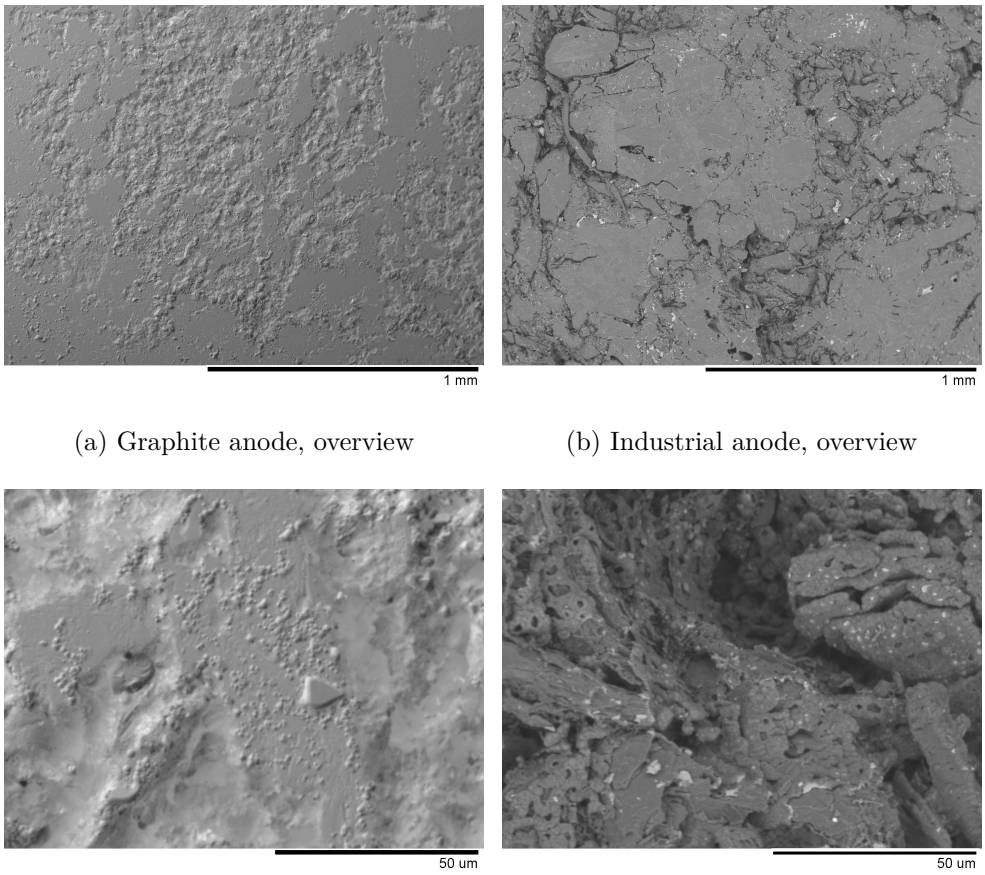

(a) Graphite anode, overview

(b) Industrial anode, overview

(c) Graphite anode, zoomed

(d) Industrial anode, zoomed on rough area

Figure 5.25: SEM images of surface of graphite and industrial vertical anodes after one hour of anode effect on 25 V.

Conclusions

Testing wettability with this wetting apparatus gave reasonably reproducible results when the experimental procedure was kept the same. The standard deviation between three repeats of the same experiment was less than 8 % of the total range. However, the measured wettability observed varied greatly between immersion and emersion, and equilibrium values were not obtained even after 10-20 minutes. Hence, the method is most suited to observe and compare trends in wetting behavior.

Both total bubble coverage and the size of detaching bubbles decreased with increasing current density on a horizontal graphite surface. This is likely due to increased stirring of the melt at higher current densities, but parts of the improvement may also have come from improved wetting.

The improvements in wetting of carbon anodes from normal polarizations occurred already during polarization. When the anode initially had undergone anode effect and was strongly dewetting, it would seem that much of the improvement in wettability happened instantaneously at the start of polarization. Even so, improvements in wetting were still observed after several minutes of polarization. After polarization, the wettability appeared to stay constant, if no other voltages were applied.

During anode effect, the wetting was diminished to the minimum value within a few seconds, long before any substantial surface polishing had taken place. This would suggest that the changes in wettability were not related to smoothness of the anode surface, but rather to creation of CF-bonds on the surface. The reduction in wettability after anode effect was much faster than the improvement in wettability for normal operating voltages, which suggests that removing these bonds is a somewhat slower process.

Testing with industrial anodes and glassy carbon anodes showed that these materials followed the same general trends in behavior as the graphite anodes do, despite having very different surface structures. For industrial anodes, the wettability was very similar to the graphite anodes, while the glassy carbon anodes were able to withstand much higher voltages before running into anode effect. The glassy carbon anode also recovered wettability after anode effects much faster.

To summarize, it would appear that the structure of the anode surface had very little effect on the wettability, as the changes to wettability occurred faster than the changes to

surface structure. Hence, it seems likely that most of the observed change in wettability is due to chemical bonds on the surface.

Further work

Several experiments could be conducted building on this thesis. Some of the experiments that would be possible are described below:

- **Improving procedure:** The set-up with an argon atmosphere and nearly no aluminium present under the melt is simple, but not a too realistic replica of an industrial cell. Redoing some of the experiments in an atmosphere of CO/CO_2 and possibly with aluminium present under the melt would be interesting, to see if this changes the wetting behavior. It would also be interesting to test various types of industrial anodes, to see if any differences can be detected.
- **Confirming results on bubble formation on horizontal anodes:** The experiment done on bubble formation during polarization was not sufficient to determine whether the changes in bubble size and bubble coverage stemmed only from different current density or partly from the changes to wettability. To test the effect of current density only, one could precondition the anode to a stable, good wettability before conducting the experiment.
- **Removing CF-bonds:** If there are CF-bonds present on the anode surface after extended anode effect, it would be interesting to see if some wettability could be regained by chemically removing these. How this could be done is unclear, however some compounds containing fluorine (ClF_3/OF_2) are known to react with CF-bonds at elevated temperatures [38]. It should be noted that both these compounds decompose at temperatures above approximately 200 °C, so this operation would require first extracting and cooling the anode. If one could show a difference in wettability before and after treatment with these gases, it would be a clear indication that the changes to wettability are caused by surface compounds on the anode.
- **Wetting after short electrolysis:** The work on meniscus movement on vertical anodes suggested that much of the improvement in wettability occurs during the first few seconds of polarization. However, as bubbles were still present on the surface, it is difficult to assess exactly how much the wettability improved in the first seconds. Hence, it would be interesting to do an experiment similar to the short anode effect tests. By taking an anode which has previously undergone extended anode effect and then polarizing at operating voltage for increasing length of time,

it would be possible to better assert how the duration of polarization affects the wettability.

- **Recovery after anode effects:** This work showed that changes in wettability occurs already after a few seconds of anode effect. It would however be interesting to study how the recovery after anode effect varies with varying anode effect durations. This could for instance be done by measuring the polarization time required to obtain a stable good wettability after anode effects of different durations, and to see if the maximum wetting weight is affected by the duration of anode effect previously endured.

Bibliography

[1] K. Grjotheim, C. Krohn, M. Malinovsky, K. Matiasovsky, and J. Thonstad. *Aluminium Electrolysis. Fundamentals of the Hall-Heroult Process.* Aluminium-Verlag, 1982.

[2] S. Prasad. *Studies on the Hall-Heroult aluminum electrowinning process.* Journal of the Brazilian Chemical Society, 11:245–251, 2000.

[3] K. Grjotheim, H. Kvande, and Q. Zhuxian. *Key improvements to Hall-Héroult since the end of world war II.* JOM, 47(11):32–35, 1995.

[4] M. A. Cooksey, M. P. Taylor, and J. J. J. Chen. *Resistance due to gas bubbles in aluminum reduction cells.* Jom, 60(2):51–57, 2008.

[5] R. Huglen and H. Kvande. *Global considerations of aluminum electrolysis on energy and the environment.* Light Metals: Proceedings of Sessions, TMS Annual Meeting (Warrendale, Pennsylvania), pages 373–380, 1994.

[6] IPPC. *Climate change 2007 : the physical science basis : contribution of Working Group I to the fourth assessment report of the Intergovernmental Panel on Climate Change.* Cambridge University Press, Cambridge, 2007.

[7] D. R. Sadoway. *Inert anodes for the Hall-Heroult cell: The ultimate materials challenge.* JOM, 53(5):34–35, 2001.

[8] D. S. Wong, P. Fraser, P. Lavoie, and J. Kim. *PFC emissions from detected versus nondetected anode effects in the aluminum industry.* JOM, 2015.

[9] J. Thonstad, T. A. Utigard, and H. Vogt. *On the Anode Effect in Aluminum Electrolysis.* Light Metals 2013, volume 2, pages 131–138, 2013.

[10] I. Eidsvaag. *The influence of polarization on the wetting of anodes in the Hall-Heróult process.* Specialization Project, 2015.

[11] Y. Yuan, and T. R. Lee. *Contact Angle and Wetting Properties*, pages 3–34. Springer-Verlag Berlin Heidelberg, 2013.

[12] V. M. Starov, M. G. Velarde, and C. J. Radke. *Wetting and spreading dynamics.* Surfactant science series. CRC Press, Boca Raton, 2007.

[13] A. M. Martinez, O. Paulsen, A. Solheim, H. Gudbrandsen, and I. Eick. *Wetting between carbon and cryolitic melts. Part I: Theory and equipment.* Light Metals 2015, pages 665– 670, 2015.

[14] W. E. Haupin. *Principles of Aluminum Electrolysis.* Light Metals 2013.

[15] J. Thonstad, P. Fellner, G. M. Haarberg, J. Hives, H. Kvande, Å. Sterten. *Aluminium Electrolysis - Fundamentals of the Hall-Heroult Process.* Aluminium-Verlag, Düsseldorf, 2001.

[16] B. Lillebuen, S. A. Ytterdahl, R. Huglen, and K. A. Paulsen. *Current efficiency and back reaction in aluminium electrolysis.* Electrochimica Acta, 1980.

[17] L. Cassayre, P. Palau, P. Chamelot, and L. Massot. *Properties of low-temperature melting electrolytes for the aluminum electrolysis process: A review.* Journal of Chemical & Engineering Data, 55(11):4549–4560, 2010.

[18] P. Meunier, B. Welch, M. Skyllas-Kazacos, and V. Sahajwalla. *Effect of dopants on wetting properties and electrochemical behaviour of graphite anodes in molten Al2O3-cryolite melts.* Journal of Applied Electrochemistry, 39(6):837–847, 2009.

[19] R. J. Thorne, C. Sommerseth, A. M. Svensson, E. Sandnes, L. P. Lossius, H. Linga and A. P. Ratvik. *Understanding Anode Overpotential.* Light Metals 2014, pages 1213-1217, 2014.

[20] R. J. Thorne, C. Sommerseth, A. P. Ratvik, S. Rorvik, E. Sandnes, L. P. Lossius, H. Linga, and A. M. Svensson. *Bubble Evolution and Anode Surface Properties in Aluminium Electrolysis.* Journal of the Electrochemical Society, 162(8):E104–E114, 2015.

[21] Z. Zhao, Z. Wang, B. Gao, Y. Feng, Z. Shi, and X. Hu. *Observation of Anodic Bubble Behaviors Using Laboratory Scale Transparent Aluminium Electrolysis Cells.* John Wiley & Sons, Inc., 2015.

[22] D. C. Chesonis, and A. F. Lacamera. *The influence of gas-driven circulation on alumina distribution and interface motion in a Hall-Heroult cell.* Light Metals 1990, pages 211–220, 1990.

[23] H. Vogt. *Contribution to the interpretation of the anode effect.* Electrochimica Acta, 42(17):2695–2705, 1997.

[24] L. Cassayre, T. A. Utigard, and S. Bouvet. *Visualizing gas evolution on graphite and oxygen-evolving anodes.* Jom-Journal of the Minerals Metals & Materials Society, 54(5):41–45, 2002.

[25] L. Cassayre, G. Plascencia, T. Marin, S. Fan, and T. Utigard. *Gas evolution on graphite and oxygen-evolving anodes during aluminium electrolysis.* Light Metals 2006, Vol 2: Aluminum Reduction Technology, pages 379–383, 2006.

[26] A. Solheim, H. Gudbrandsen, A. M. Martinez, K. E. Einarsrud, and I. Eick. *Wetting between Carbon and Cryolitic melts. Part II: Effect of Bath Properties and Polarisation.* Light Metal 2015, pages 671–676, 2015.

[27] E. Lae, V. Sahajwalla, B. Welch, and M. Skyllas-Kazacos. *Influence of oxide dopants on the wetting of doped graphite by cryolite/alumina melts.* Journal of Applied Electrochemistry, 35(2):199–206, 2005.

[28] H. Åsheim, T. A. Aarhaug, A. Ferber, O. S. Kjos, and G. M. Haarberg. *Monitoring of Continuous PFC Formation in Small to Moderate Size Aluminium Electrolysis Cells.* John Wiley & Sons, Inc., 2014.

[29] D. S. Wong, A Tabereaux, and P. Lavoie. *Anode effect phenomena during conventional AEs, low voltage propagating AEs & non-propagating AEs.* Light Metals 2014, 2014.

[30] J. Marks, and C. Bayliss. *GHG measurement and inventory for aluminum production.* Light Metals 2012, pages 805–808, 2012.

[31] R. G. Haverkamp, and B. C. C. Cowie. *C K-edge NEXAFS study of fluorocarbon formation on carbon anodes in molten NaF-AlF3-CaF2.* Surface and Interface Analysis, 45(13):1854–1858, 2013.

[32] R. G. Haverkamp. *An XPS study of the fluorination of carbon anodes in molten NaF-AlF3-CaF2.* Journal of Materials Science, 47(3):1262–1267, 2012.

[33] F. C. Cowlard, and J. C. Lewis. *Vitreous carbon - a new form of carbon.* Journal of Materials Science, 2(6):507–512, 1967.

[34] J. Zoric, and A. Solheim. *On gas bubbles in industrial aluminium cells with prebaked anodes and their influence on the current distribution.* Journal of Applied Electrochemistry, 30(7):787–794, 2000.

[35] R. K. Jain, S. B. Tricklebank, and B. Welch. *Interaction of aluminas with aluminium smelting electrolytes.* Light Metals 1983, 1983.

[36] X. W. Wang. *Alumina dissolution in aluminum smelting electrolyte.* Light Metals 2009, pages 383–388, 2009.

[37] B. J. Welch. *Aluminum production paths in the new millennium.* Jom-Journal of the Minerals Metals & Materials Society, 51(5):24–28, 1999.

[38] S. Ebnesajjad. *Fluoroplastics, Volume 1, 2nd Edition. Non-Melt Processible Fluoropolymers - The Definitive User's Guide and Data Book.* Plastics Design Library, Norwich, NY, 2014.